Chapter 3

RESULTS AND DISCUSSION

3. Results and Discussion

This chapter has been subdivided into four different sections as mentioned below

1. Two-stage leaching from obsolete mobile phone PCBs: Extraction of copper, nickel and gold
2. Separation of copper and nickel from stage-1 leach solution
3. Separation of gold and silver from stage-2 leach solution
4. Validation of two-stage leaching through Response Surface Methodology (RSM) - A DOE study

Section-1

Two-stage leaching from obsolete mobile phone PCBs: Extraction of copper, nickel and gold

3.1. Two-stage leaching from obsolete mobile phone PCBs: Extraction of copper, nickel and gold

In this section, a two-stage leaching process is developed for the sequential recovery of copper, nickel and gold from the metal clads of obsolete mobile phone PCBs. As the presence of base metals impacts upon the leaching of precious metals [29], [83], the selective dissolution of copper and nickel over gold is targeted first using aqueous leach solutions. Moreover, reports on the sequential recovery of base and precious metals from WPCBs is limited. In stage-1, the dissolution of copper and nickel was observed to facilitate the isolation of a gold-rich residue. In stage-2, selective extraction of gold was observed from the residue obtained in stage-1 leaching. Optimization of leaching parameters such as time, temperature, type of leachant, concentration of leachant, pulp density and agitation speed were also observed in both stages. Finally, the kinetics of leaching of copper, nickel and gold were studied to calculate experimental activation energies.

3.1.1. Stage-1 leaching: Dissolution of copper, nickel and isolation of gold

The metallic portion produced in the pre-treatment process is dissolved in various aqueous leaching reagents such as sulfuric acid, nitric acid and the combination of sulfuric and nitric acids in order to study the efficacy of leachant and the optimization of leaching of copper and nickel. Experiments are started with sulfuric acid as a leachant.

3.1.1.1. Sulfuric acid leaching

Initially, leaching experiments with various concentrations of sulfuric acid (1-3 M) were undertaken at 30 °C for 3 h ,with a pulp density of 50 g/L and a stirring speed of 500 rpm. These results demonstrate that the percentage dissolution of copper, nickel, and gold increases with increasing concentration of sulfuric acid but the overall leaching efficiency

is limited to < 9% of the total amount of metal present in all cases. In addition, no selectivity in leaching is observed, with various amounts of all three metals being dissolved as shown in **Figure 3.1**. As such, acid concentration was restricted to 3 M as this helps in the downstream purification stages and limits acid splashing.

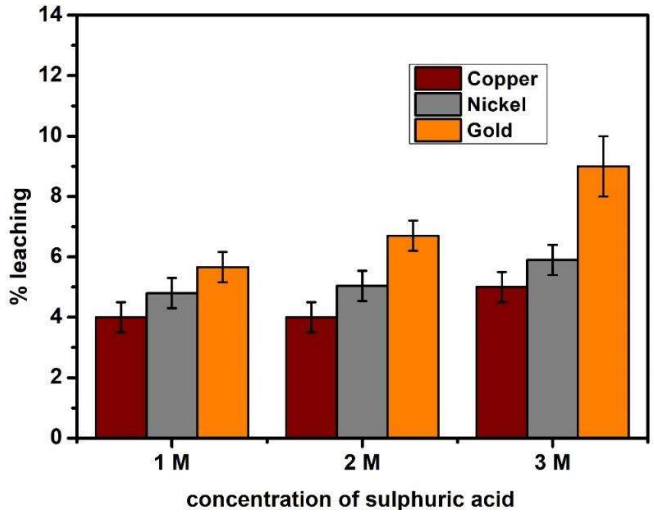

Figure 3.1- Effect of concentration of sulfuric acid on leaching of copper, nickel and gold [Temp. 30 °C; time 3 h; stirring speed 500 rpm; pulp density 50 g/L]

As the metals present in WPCBs are in their metallic form, the above set of leaching experiments confirmed the need for the addition of an oxidant to facilitate effective leaching [86]. As nitric acid has proved to be a more proficient oxidant than hydrogen peroxide [31], [168], 1 M nitric acid was added to various concentrations of sulfuric acid at 30 °C by keeping the other parameters constant. The percentage of copper and nickel leaching is observed in **Figure 3.2 (a) and (b)**. It is observed that the leaching of copper and nickel increased with increasing concentration of sulfuric acid, and optimum dissolution is observed using 3 M sulfuric acid with 1 M nitric acid. However, some gold leaching (14%) is also seen **(Figure 3.2 (c))** and so this leaching method was discounted due to its negative impact on a clean two-stage, sequential metal separation.

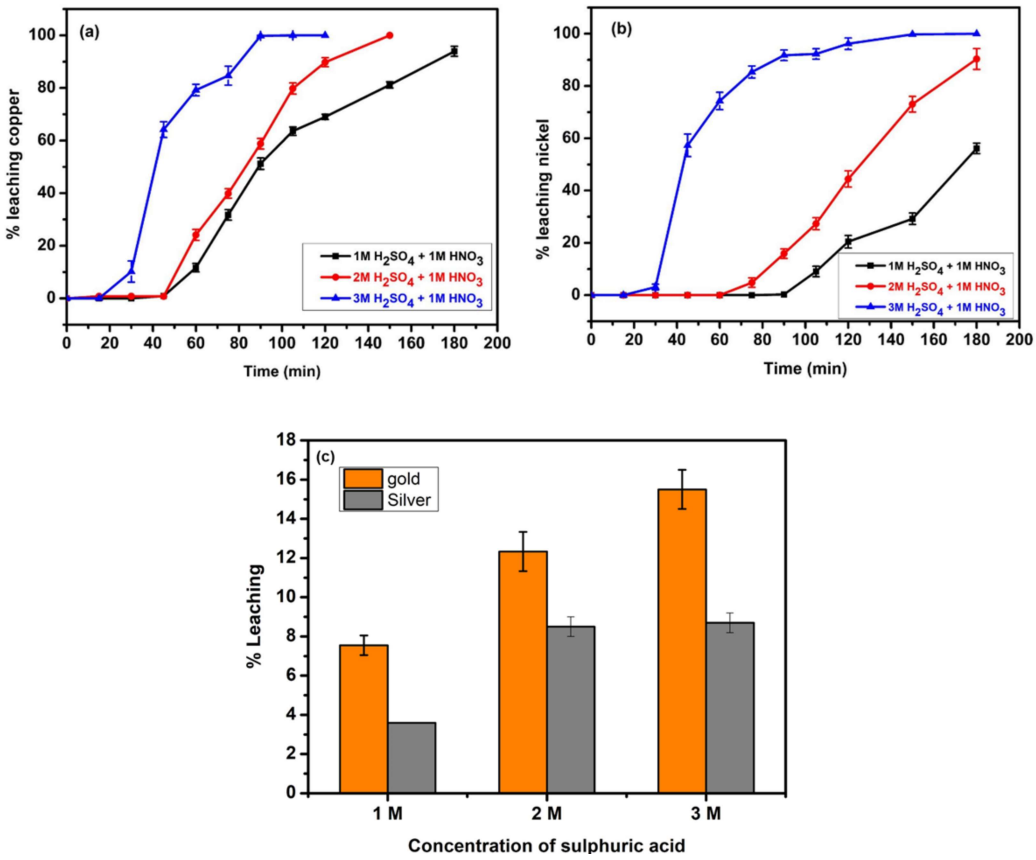

Figure 3.2- Effect of addition of 1 M nitric acid on leaching of (a) copper and (b) nickel (c) gold and silver [Temp. 30 °C; time 3 h; stirring speed 500 rpm; pulp density 50 g/L]

3.1.1.2. Nitric acid leaching

The lack of selectivity in the above leaching stages led us to explore the use of nitric acid as a single leaching agent for copper and nickel only, as previous reports have demonstrated that 2-5 M nitric acid is an effective solvent for the dissolution of copper (88.5-99.9%) from shredded WPCBs [2].

i) Effect of concentration of nitric acid

Three leaching experiments were conducted using 1-3 M nitric acid at 30 °C, for 3 h, at a 50 g/L pulp density and 500 rpm stirring speed. These experiments show a gradual increase in copper and nickel content in the leach liquor on increasing the acid

concentration from 1 to 3 M. Quantitative leaching of copper and nickel is observed using 3 M nitric acid over 2 h (**Figure 3.3 (a) and (b)**), with some gold dissolution only occurring after 2 h (**Figure 3(c)**). Lower concentrations of nitric acid in the leach liquor are favourable for downstream separations such as solvent extraction. Based on these results, leaching with 3 M nitric acid for 2 h appears to be the most effective method for the effective leaching of copper and nickel.

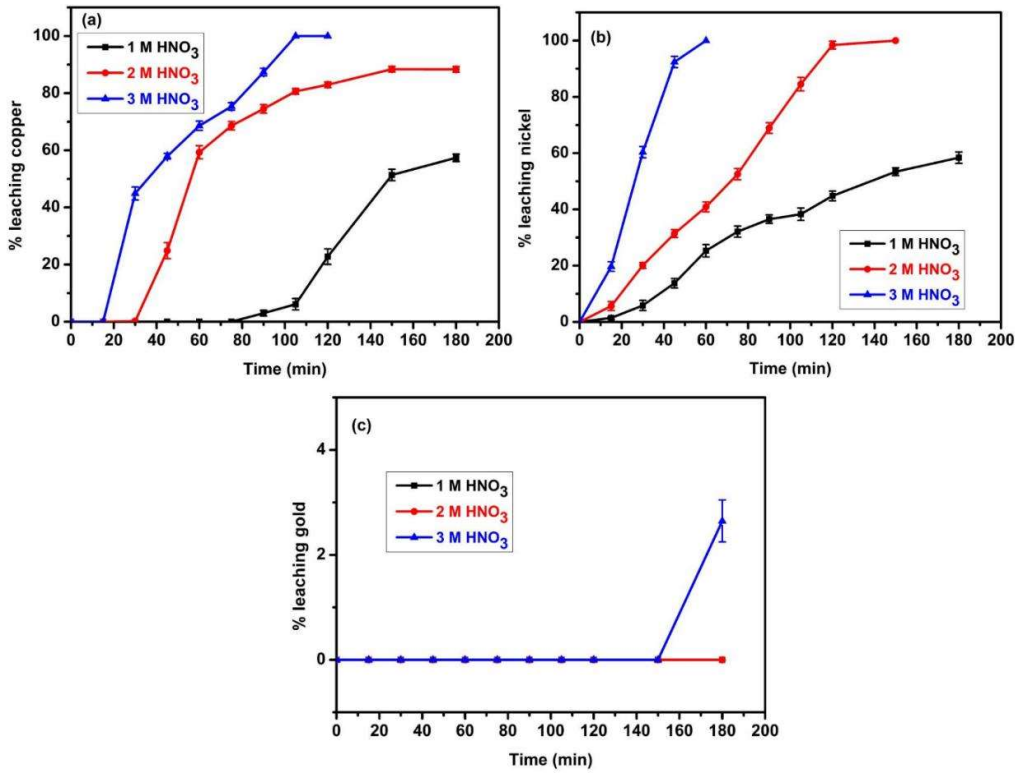

Figure 3.3- Effect of concentration of nitric acid on (a) copper, (b) nickel and (c) gold leaching [Temp. 30 °C; time 3 h; stirring speed 500 rpm; pulp density 50 g/L] [169]

ii) Effect of temperature

The effect of temperature on the dissolution of copper and nickel was examined by varying it from 30 to 60 °C under the optimized concentration of nitric acid (3 M) and time (2 h). Other parameters are 50 g/L pulp density and 500 rpm stirring speed. These experiments show that copper and nickel leaching increases with increasing the

temperature and complete leaching of these metals is observed in all cases, albeit with a reduction in residence time as shown in **Figure 3.4(a) and (b)**. In addition, gold leaching accelerates from 40 °C and above **(Figure 3.4(c))**. Therefore 30 °C was identified as the optimal temperature to maximize copper and nickel leaching while minimizing gold dissolution.

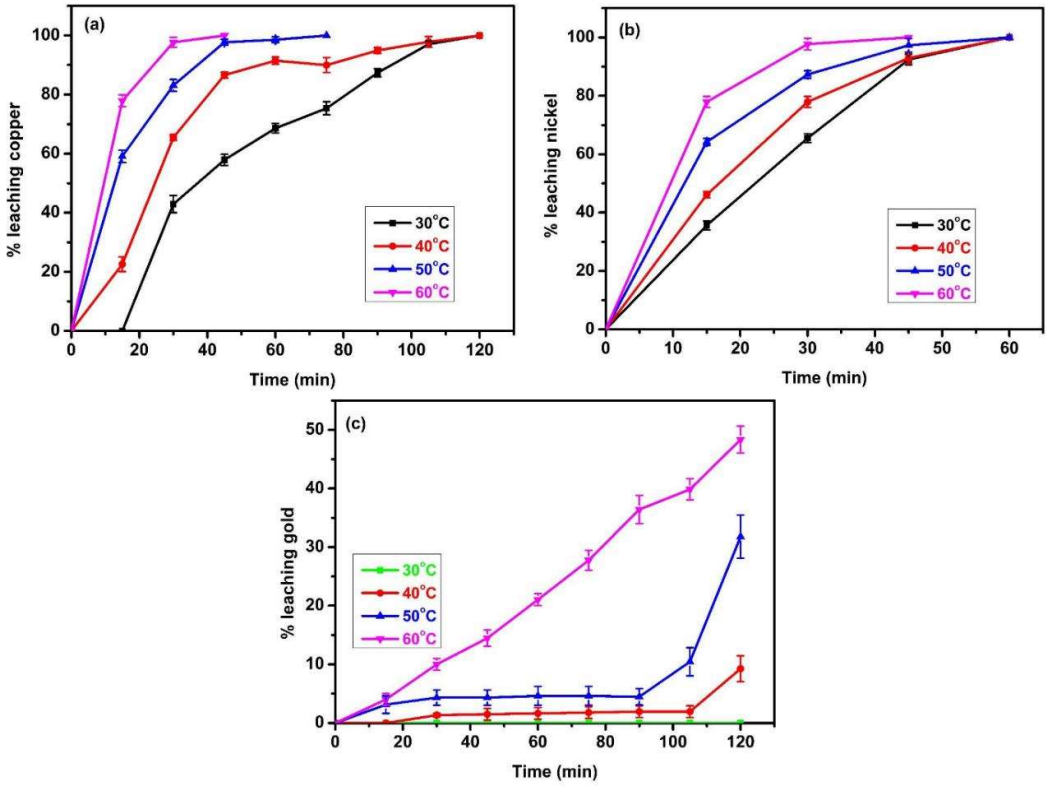

Figure 3.4- Effect of temperature on nitric acid leaching of (a) copper, (b) nickel and (c) gold [Concentration of nitric acid 3 M; time 2 h; stirring speed 500 rpm; pulp density 50 g/L][169]

iii) Effect of pulp density

Leaching experiments were then undertaken where the pulp density was varied from 25 g/L to 100 g/L, in 3 M nitric acid, for 2 h, at 30 °C and 500 rpm stirring speed. Results are shown in **Figure 3.5 (a) and (b).** A gradual increase in copper and nickel leaching is observed with increasing pulp density until 50 g/L, and a slight decrease in the

concentration of copper and nickel is observed at higher pulp density (75 and 100 g/L). It is evident that these higher pulp densities result in insufficient mass transfer, similar to that seen by Chen and co-workers [170] and a decrease in residual acid concentration [31].

Similarly, the leaching of gold is negligible at 25 g/L and 50 g/L as shown in **Figure 3.5 (c)**, the higher pulp density of 50 g/L appears to be the optimal parameter for the selective and complete leaching of copper and nickel without gold dissolution.

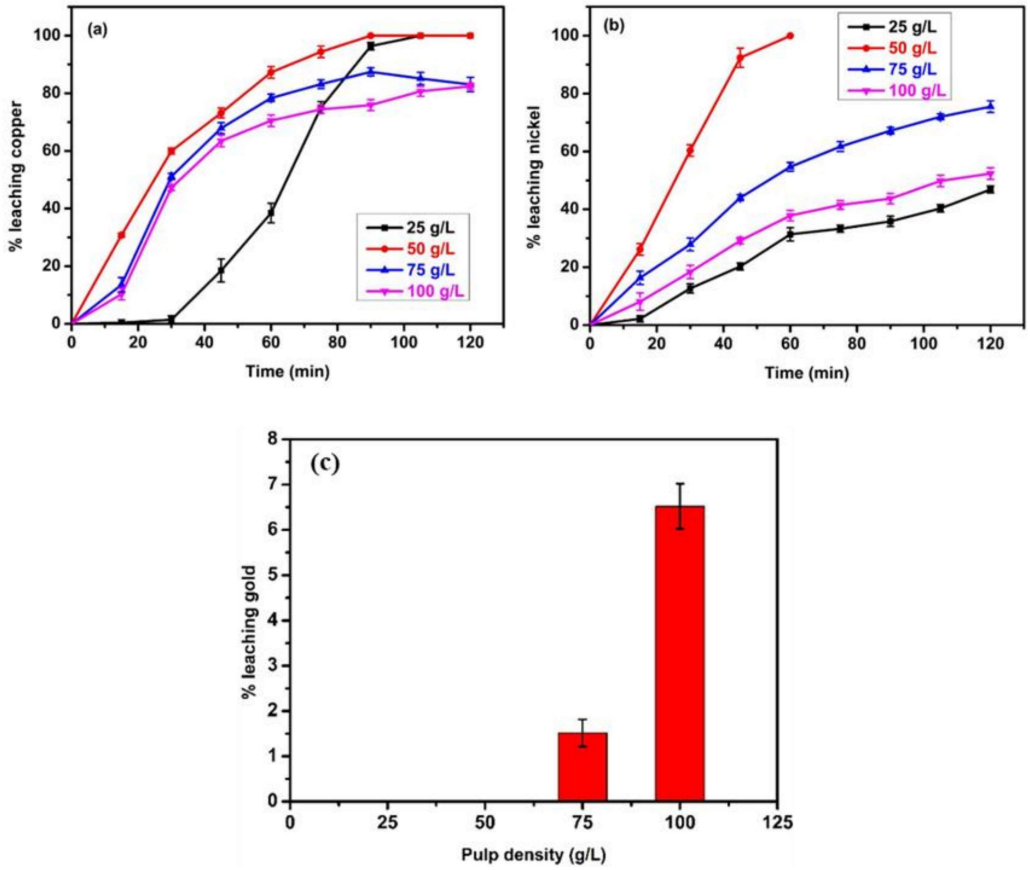

Figure 3.5- Effect of pulp density on leaching of (a) copper (b) nickel and (c) gold [Temp. 30 °C; time 2 h; stirring speed 500 rpm; concentration of nitric acid 3 M] [169]

iv) Effect of stirring speed

Finally, the stirring speed was varied between 100-500 rpm using 3 M nitric acid with a 2 h residence time, 50 g/L pulp density and at 30 °C temperature. The experiments show that the leaching of copper and nickel increases slightly with increasing stirring speed **(Figure 3.6).** In addition, no gold leaching is observed in all three cases. At higher agitation speeds (>500 rpm), considerable splashing of the acid is observed, with the metallic materials adhering to the upper portion of the reactor. For these reasons the 500 rpm stirring speed was selected as the optimal value for leaching.

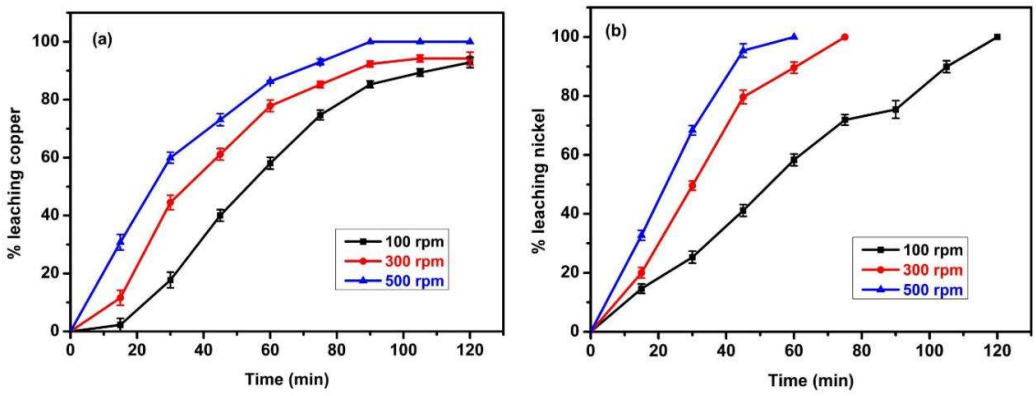

Figure 3.6- Effect of stirring speed on leaching of (a) copper and (b) nickel [Temp. 30 °C; time 2 h; concentration of nitric acid 3 M; pulp density 50 g/L] [169]

From these studies, the optimized parameters for the effective leaching of copper and nickel are mentioned as 3 M nitric acid; 30 °C temperature; 2 h residence time; 50 g/L pulp density and agitation speed of 500 rpm. Along with copper and nickel, other elements such as zinc (99.5%), lead (99.3%), cadmium (99.9%), aluminium (99.3%), palladium (99.9%), and to a lesser extent tin (30.8%) and silver (8%) are also dissolved at these optimized parameters **(Figure 3.7)**. Importantly, gold is not dissolved and remains in the residue. In this process, significant amounts of NO_x gases were produced when using higher concentrations of nitric acid as shown in Eq. 3.1-3.3, which would

have to be scrubbed and recycled into fresh nitric acid to be environmentally sustainable [171].

$$Cu + 4HNO_3 \rightarrow Cu(NO_3)_2 + 2H_2O + 2NO_2 \quad (3.1)$$

$$3Cu + 8HNO_3 \rightarrow 3Cu(NO_3)_2 + 4H_2O + 2NO \quad (3.2)$$

$$Ni + 4HNO_3 \rightarrow Ni(NO_3)_2 + 2H_2O + 2NO_2 \quad (3.3)$$

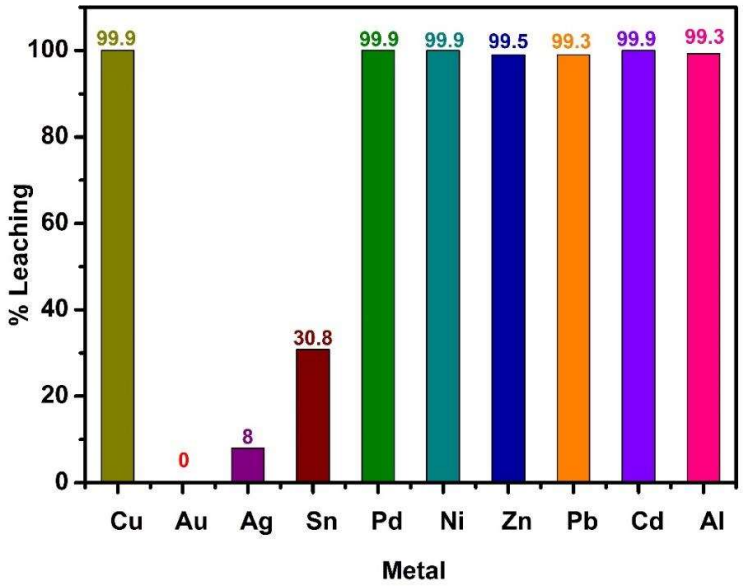

Figure 3.7- Leaching efficiency of various metals in stage-1 leaching [Temp. 30 °C; time 2 h; concentration of nitric acid 3 M; pulp density 50 g/L; stirring speed 500 rpm] [112]

Chemical analysis of the filtered leach solution at the optimized parameters revealed that it comprises 97.4 ± 1 wt% copper and 0.7 ± 0.1 wt% nickel, along with zinc (0.5 ± 0.2 wt%), lead (0.5 ± 0.1 wt%), cadmium (0.5 ± 0.2 wt%), aluminium (0.02 wt%) and tin (0.4 ± 0.1 wt%) as minor quantities (**Figure 3.8**). The leach liquor has been purified to separate individual metals with various purification processes such as solvent extraction and cementation. A detailed explanation of the separation processes has been mentioned in the coming sections (section 3.2).

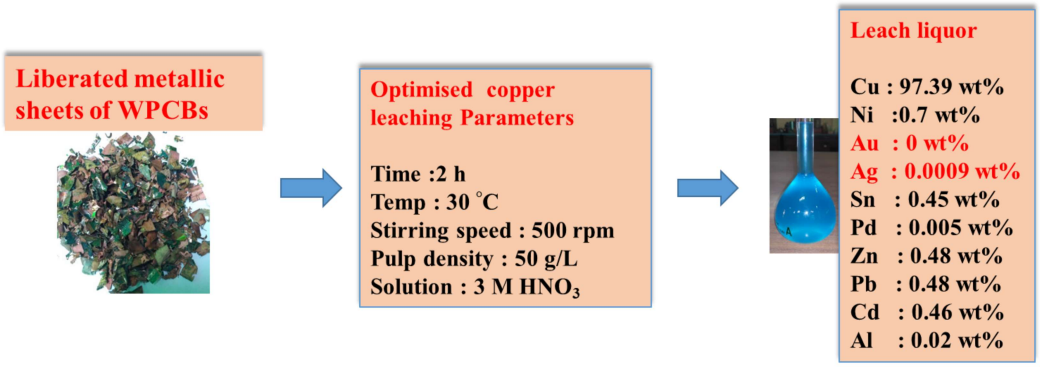

Figure 3.8- Chemical analysis of stage-1 Leach solution at optimized parameters

3.1.1.3. Analysis of stage-1 leach residue

The separated residue was initially analyzed with SEM-EDS as shown in **Figure 3.9**. The figure shows that the residue consists of a dominant non-metallic fraction along with tin, gold and other traces. To find out the accurate metallic fraction, it is subsequently dissolved in aqua regia and analyzed by AAS, which revealed that negligible quantities of copper remained (0.003 ± 0.001 wt.%), while the other components were Au (0.05 ± 0.01 wt%), Ag (0.025 ± 0.01 wt%) and Sn (0.7 ± 0.1 wt%) along with a major non-metallic fraction.

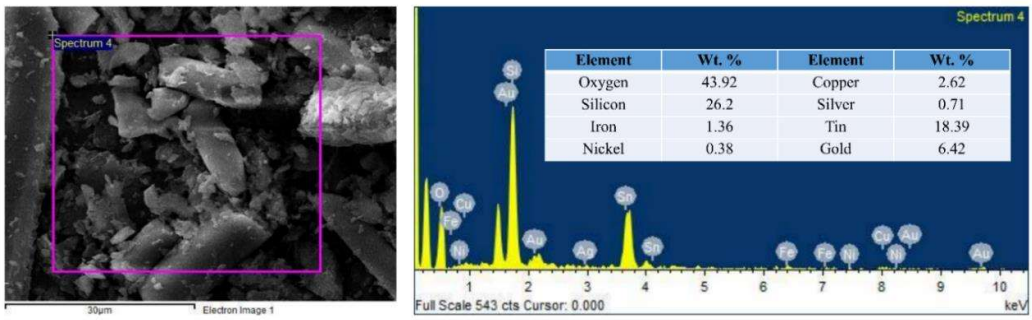

Figure 3.9- SEM-EDS of leach residue obtained in stage-1 leaching

3.1.1.4. Kinetic study of leaching of copper and nickel

The kinetics of leaching is important to study the mechanism of dissolution of copper and nickel from the separated metallic layers of WPCBs. Usually, in the leaching process, the leaching reagent reacts with the mineral particle in several sequential steps. They are

a) Diffusion of reagent from the liquid phase (bulk) to the porous liquid boundary film
b) Diffusion through the porous layer
c) Reaction of the reagent with the mineral surface forms new products.
d) Diffusion of the product metal through the porous layer
e) Diffusion of the product metal away from the surface

Based on the nature of a solid-liquid reaction, several models can be discussed, and among them, the popular shrinking core model is the most applied one [172]. From the above mentioned several sequential steps of a heterogeneous reaction, the slowest step controls the rate of a reaction. If the diffusion is much faster than the reaction, then the model would be reaction-controlled and vice versa. In addition, from the activation energy point of view, when it is less than 3 kcal/mol, suggested diffusion controlled while greater activation energy indicates chemical reaction controlled model.

In order to determine the kinetic parameters of a reaction in the leaching of copper and nickel, the shrinking-core model was applied by analyzing the experimental percentage leaching versus time at different temperatures. In a solid-liquid reaction system, the reactions are usually controlled by diffusion through the product layer or chemical reaction at the surface of a material. If the reaction is controlled by the diffusion through the product layer then Eq. 3.4 holds [173],

$$1-2/3x-(1-x)^{2/3} = k_d t \quad (3.4)$$

whereas if the reaction is controlled chemically by a surface reaction then Eq. 3.5 holds [174].

$$1-(1-x)^{1/3} = k_c t \qquad (3.5)$$

where x is fraction of leaching, k_d is kinetic rate constant for the diffusion-controlled reaction, k_c is kinetic rate constant for surface-controlled reaction, and t is reaction time (min).

Analysis of the experimental data using the above kinetic equations display a good and almost similar linear fitting to all of the parameters for the optimisation of leaching of copper and nickel using the both diffusion and chemically controlled surface-reaction model (**Figure 3.10**). Based on these R^2 values, the fit for the diffusion controlled model is not significantly poorer than the fit for the surface-reaction controlled model. Therefore the range of experimental activation energy is calculated to assess the kinetic model of the reaction (**Figure 3.11**).

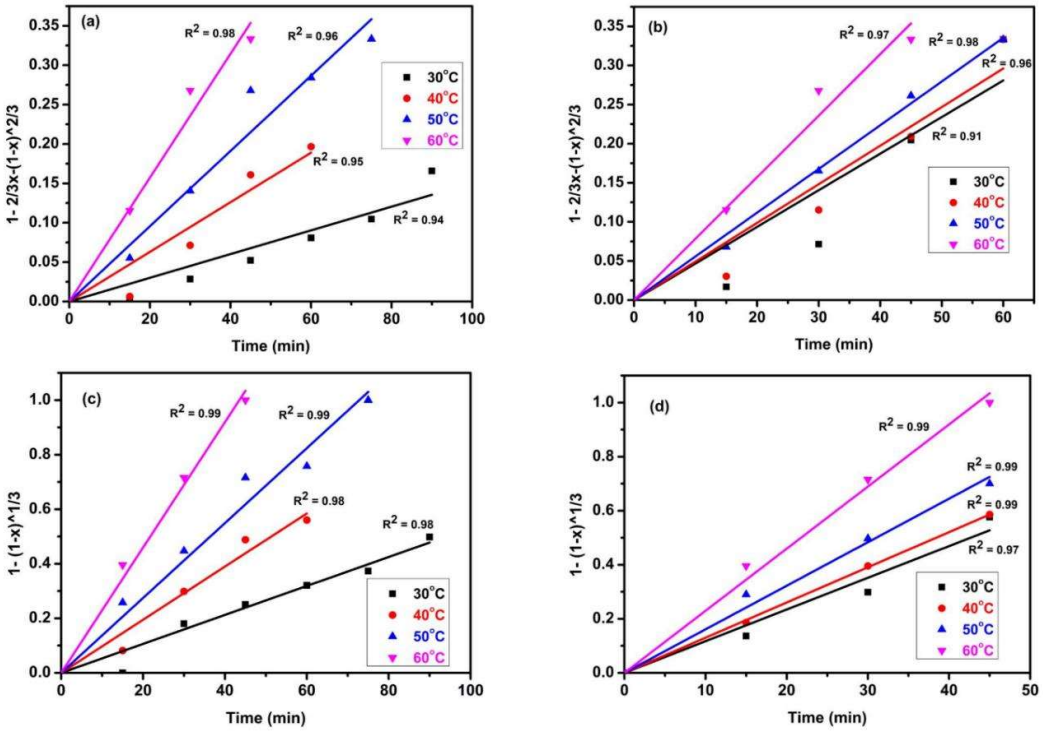

Figure 3.10- Kinetics plots for (a) diffusion controlled model for leaching of copper (b) diffusion controlled model for leaching of nickel (c) reaction controlled model for leaching of copper (d) reaction controlled model for leaching of nickel using optimal

leaching conditions [Concentration of nitric acid 3 M; pulp density 50 g/L; stirring speed 500 rpm] [169]

For the calculation of experimental activation energy (E_a), k_c and k_d were determined from the slopes of the linear plots (**Figure 3.10**) and expressed with respect to the Arrhenius equation [175].

$$k = A\, e^{(-Ea/RT)} \qquad (3.6)$$

where k is the reaction rate constant, A is the pre-exponential factor, E_a is the activation energy, and R is the gas constant (8.314 J K^{-1} mol^{-1}). Analysing the data generates calculated activation energies for copper leaching from diffusion and reaction model of 39.7, 45.1 kJ/mol, and for nickel leaching of 18.4, 15.8 kJ/mol that fall in the range expected for the chemically controlled reaction model. Typically E_a is 1-3 kcal/mol (4.18-12.55 kJ/mol) for diffusion controlled model and higher for chemically controlled surface reaction model [176], [177]. Higher activation energies are observed in the reaction controlled model because the required energy for the chemical reaction that occurred at the surface of the metal particles is higher than the energy for the diffusion of the reactant at the interface.

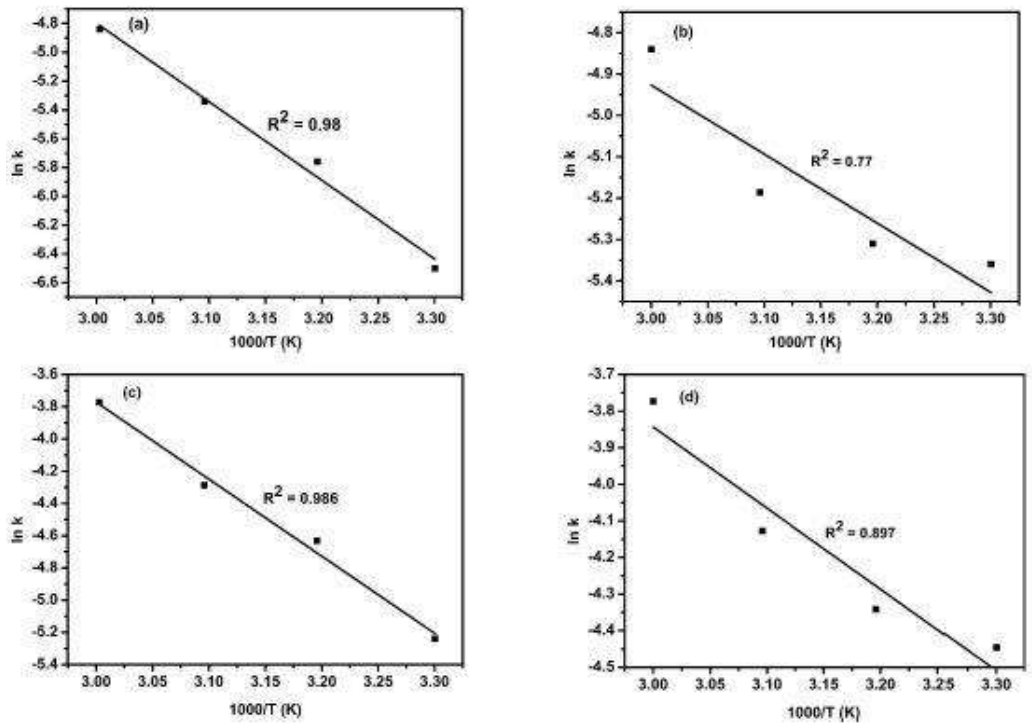

Figure 3.11- Arrhenius plots for (a) leaching of copper in diffusion controlled model (b) leaching of nickel in diffusion controlled model (c) leaching of copper in reaction controlled model (d) leaching of nickel in reaction controlled model from WPCBs using optimal leaching conditions [169]

3.1.2. *Stage-2 leaching: Dissolution of gold*

Stage-2 leaching studies were evaluated by dissolving the residue that arose from the first stage leaching in an aqueous halide solution. Halide leaching is an alternative to conventional gold leaching techniques (see chapter1, introduction) and in that, chlorine or bromine are generated *in situ* by the chemical reaction between acidic reagent and sodium halides and acts as a strong oxidizing agent for the effective leaching of gold (Eq. 3.9). Studies of reduction potential (Eh) vs pH diagram for the feasibility of gold in halide solution revealed that leaching of gold is possible [162]–[164]. However, the chlorination leaching method has disadvantages remain, difficult to control in chlorine gas released, and the corrosion problems [178]. Similarly, in the case of iodine also higher consumption of leaching reagent occurs [163]. On the other hand, in bromine leaching,

the generation of stabilized bromine which has lower vapour pressure than liquid bromine, is achieved higher gold recovery from conventional ores [179]. In bromine medium, the gold is oxidized by bromine and stabilized as the gold bromide complex, as represented in Eq. 3.7 and Eq. 3.8.

$$Br_2 + 2e^- \rightarrow 2Br^- \quad (3.7)$$

$$Au + 4Br^- \rightarrow AuBr_4^- + 3e^- \quad (3.8)$$

$$NaBr + 2H_2SO_4 \rightarrow NaHSO_4 + Br_2 + SO_2 + 2H_2O \quad (3.9)$$

Parameters such as leaching reagent, concentration of leachant, temperature and stirring speed were studied for the effective extraction of gold.

3.1.2.1. Effect of leaching reagent

Leaching experiments were started with the effect of type of leaching reagent on gold dissolution at 50 °C for 2 h with 500 rpm stirring speed. Initially, 3 M sulfuric acid alone is used as a leachant. In addition to that, the effect of addition of 2 M sodium chloride and 2 M sodium bromides to the sulfuric acid on gold dissolution was also observed. The results represent that sulfuric acid alone is not a suitable leachant for gold leaching as the recovery is restricted to 7%. Similarly, the addition of 2 M sodium chloride causes increasing the percentage of leaching to 31.1%. Contrary, in the case of 2 M sodium bromide addition, the leaching percentage of gold is 88.26%. It is evident that the generation of stabilised bromine helped to increase the gold leaching. Based on these results, 3 M sulfuric acid with the combination of 2 M sodium bromide is suitable for more gold leaching at 50 °C in 2 h resident time by keeping the stirring speed at 500 rpm as shown in **Figure 3.12**.

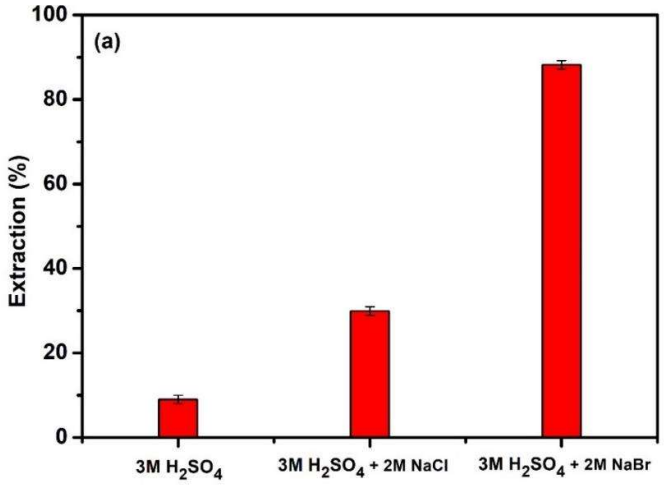

Figure 3.12- Effect of leaching reagent on gold leaching [Temp. 50 °C; time 2 h; stirring speed 500 rpm] [180]

3.1.2.2. Effect of concentration of sodium bromide in leachant

Effect of addition of 1-3 M sodium bromide to 3 M sulfuric acid on gold leaching was studied at 50 °C. Other parameters are 2 h resident time and 500 rpm stirring speed. **Figure 3.13** elucidates gold leaching gradually increased from 57% to 90% with increasing the concentration of sodium bromide from 1 M to 3 M and the rate of leaching is constant after 1 h leaching. So that, from these observations, a conclusion can be obtained that the addition of 3 M sodium bromide to 3 M sulfuric acid is an active leachant for the gold leaching in 1 hour at 50 °C with an agitation of 500 rpm.

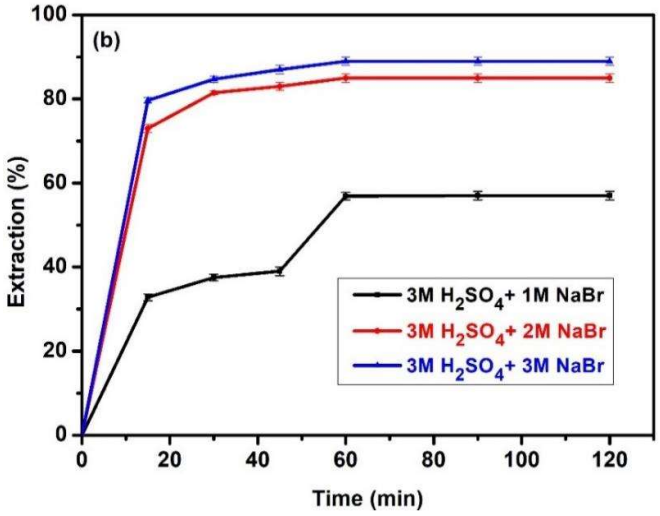

Figure 3.13- Effect of concentration of sodium bromide on gold leaching [Temp. 50 °C; time 2 h; stirring speed 500 rpm] [112]

3.1.2.3. Effect of temperature on gold leaching

The effect of temperature on gold leaching was also investigated in the range of 30 to 90 °C. The remaining parameters are 1 h resident time, 3 M sulfuric acid with 3 M sodium bromide as leaching reagent and 500 rpm agitation speed. It has been observed from **Figure 3.14** that the rate of gold leaching increased gradually from 82.25 to 95.28% by increasing the temperature from 30 to 70 °C in 1 h resident time. Contrary by increasing the temperature from 70 to 90 °C, the rate of leaching decreased to 88.48%. This is presumably due to the loss of bromine at elevated temperatures. Based on these results, 70 °C is reported as optimized temperature for the maximum and effective leaching of gold.

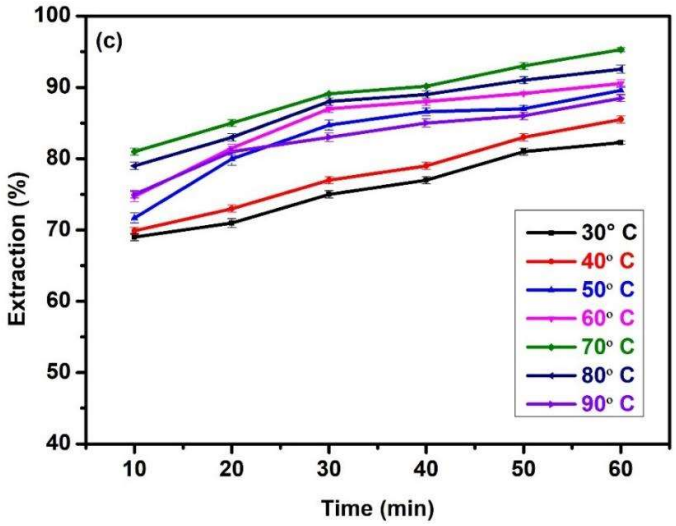

Figure 3.14- Effect of temperature on gold leaching [3 M sulfuric acid with 3 M sodium bromide; time 1 h; stirring speed 500 rpm] [112]

3.1.2.4. Effect of stirring speed

Finally, the effect of stirring speed on leaching of gold was also studied by changing it from 100 to 500 rpm with an increment of 200 rpm under the optimized conditions viz. 70 °C, 1 h resident time and 3 M sulfuric acid with 3 M sodium bromide as leachant. From **Figure 3.15**, it is observed that gold leaching efficiency is almost similar in all cases. Higher agitation (>500 rpm) causes splashing of the acid, and solid particles also get stuck on the upper portion of the reactor. Therefore, 500 rpm is used for the maximum extraction of gold.

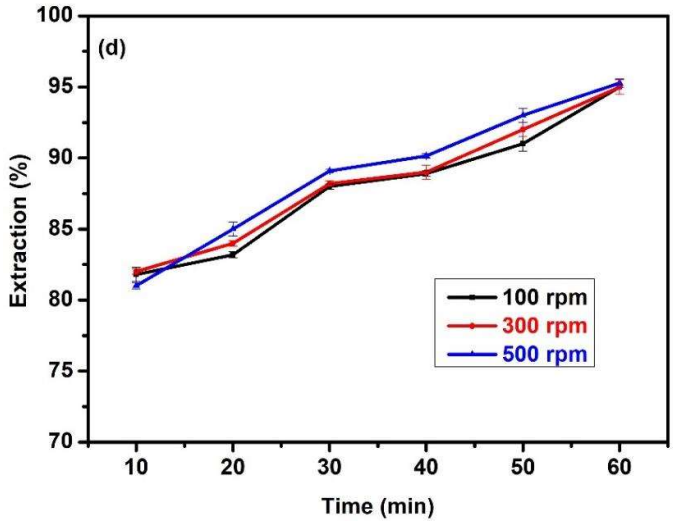

Figure 3.15- Effect of stirring speed on gold leaching [Temp. 70 °C; 3 M sulfuric acid with 3 M sodium bromide; time 1 h] [112]

Based on these studies, a conclusion can be obtained that an effective leaching of gold (95.28%) is observed at 3 M sulfuric acid with 3 M sodium bromide as leaching reagent, 1 h resident time, 70 °C temperature and 500 rpm stirring speed. In addition to gold, extraction of silver (96%) and tin (94%) was also observed at optimized parameters as presented in **Figure 3.16.**

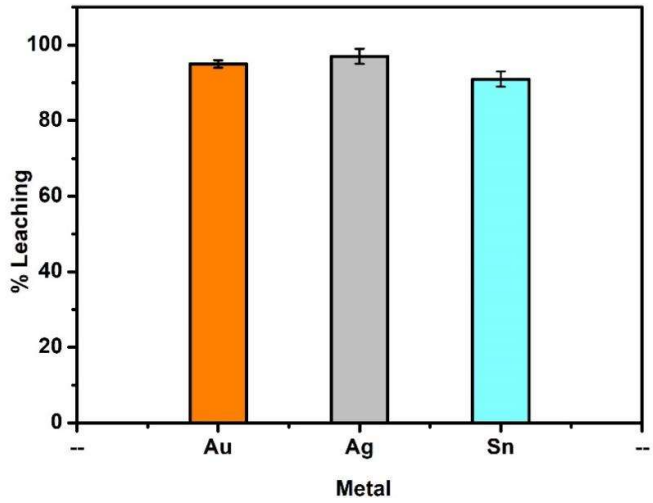

Figure 3.16- Leaching efficiency of gold, silver and tin in stage-2 leaching [Temp. 70 °C; 3 M sulfuric acid with 3 M sodium bromide; time 1 h; stirring speed 500 rpm]

Chemical analysis (ICP-OES) of the stage-2 leachate revealed that it comprises 6.36 ± 0.8 wt% gold, 91.1 ± 1.1 wt% tin, 2.16 ± 0.2 wt% silver and a minor quantity of copper (0.34 ± 0.2 wt%) as shown in **Table 3.1.** Further purification processes are required for the separation of gold, silver and tin from this leach liquor and a detailed explanation has been discussed in the coming sections (Section 3.3).

Table 3.1- Chemical analysis of stage-2 leach solution at optimized parameters

	Stage-2 Leach solution	**Error**
Element	wt%[a]	wt%
Cu	0.34	0.2
Au	6.36	0.8
Ag	2.16	0.2
Sn	91.1	1.1

[a] weight (g) of element per 100 g of residues remaining after stage-1 leach

3.1.2.5. Kinetic study of leaching of gold

To understand the nature of interaction between the gold particles and the leaching reagent, another attempt was made to fit the kinetic data obtained from the leaching experiments at different temperatures in the shrinking core models based on the diffusion and surface reaction models (see eq 3.4 and 3.5 in section 3.1.3). However, the correlation coefficients (R^2) are not more than 0.8 for the chemical and diffusion controlled models. Therefore the kinetic data was analyzed by using an emperical model (Eq. 3.10) for the leaching which is governed by logarithmic rate law.

$$-(\ln(1-(1-x))^2 = k_e t \qquad (3.10)$$

The results obtained at different temperatures give stright lines when -(ln (1-x))2 vs t is plotted and show best fit to this model which is evident from the high R^2 values as shown

in **Figure 3.17.** The best fit was observed through the emperical model may be attributed to the complex nature of the leach residue [172], [181].

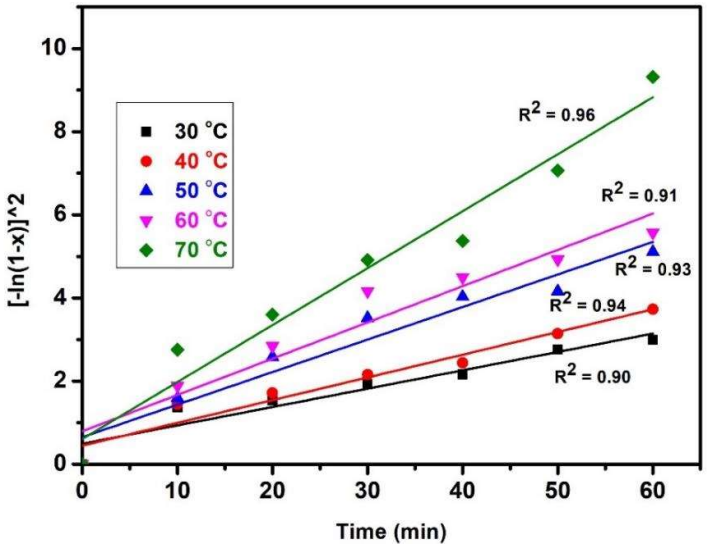

Figure 3.17- Empirical model for kinetics of leaching of gold [Temp. 30-70 °C]

Inorder to find out the activation energy (Ea), k_e was determined from the slopes of the linear plots (**Figure 3.17**) and expressed with respect to the Arrhenius equation (see eq. 3.6) with the help of a plot made between ln k vs 1/T. The plot is shown in **Figure 3.18** with a high correlation coefficient ($R^2 = 0.94$). The activation energy from the Arrhenius plot was found to be 22.76 kJ/mol.

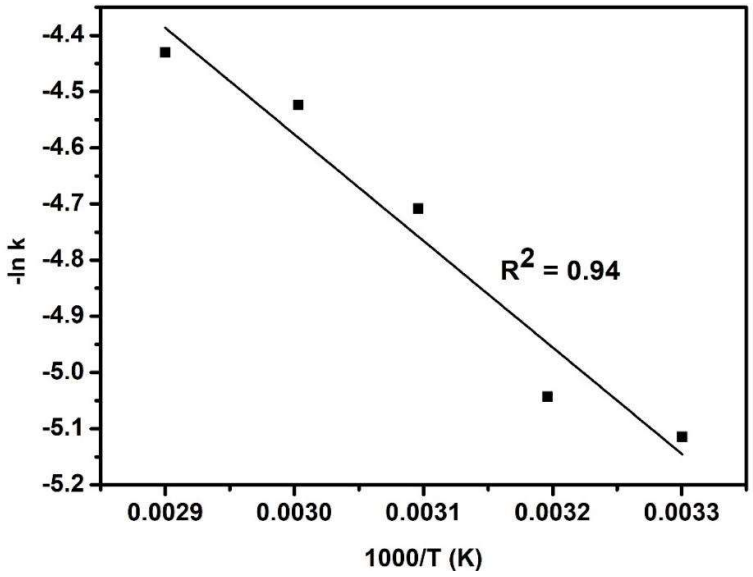

Figure 3.18- Arrhenius plot for the empirical kinetic model for gold

Conclusions

- A two-stage metal leaching process selectively dissolves copper and nickel from delaminated WPCBs in stage-1 leaching to leave a gold-rich solid residue for the subsequent extraction of gold.
- Optimal conditions for the selective leaching of copper and nickel were achieved when using 3 M nitric acid at 30 °C, over a 2 h resident time, for 50g/L pulp density, and 500 rpm agitation speed. Importantly, no gold was dissolved using these conditions.
- In stage-2 leaching selective extraction of gold is observed with halide leaching.
- Optimal conditions for the selective leaching of gold were achieved when using 3 M sulfuric acid with 3 M sodium bromide at 70 °C, over a 1 h time and 500 rpm agitation speed.

- Kinetic studies show that the activation energies calculated for copper and nickel dissolution are within the expected range for a chemically controlled dissolution model.
- Similarly, kinetic studies for stage-2 leach solution shows that it follows the logarithmic model.
- The leaching process optimized in this section avoids the need for high temperatures, reduces energy consumption and effluent generation, leading to the cleaner processing of obsolete mobile phone PCBs for the separation of copper, nickel and gold.

Section-2

Separation of copper and nickel from stage-1 leach solution

3.2. Separation of copper and nickel from stage-1 leach solution

This section explains about the optimization of the separation and recovery of copper and nickel from stage-1 leach liquor through two-stage solvent extraction. Copper was selectively extracted in stage-1 solvent extraction (SX1) by leaving nickel rich raffinate. In stage-2 solvent extraction (SX2), selective recovery of nickel was studied from the other minor base metals. Salicylaldehide derived "salox" ligand, ACORGA M5640 was used as a significant extractant or carrier diluted in kerosene as an organic solvent in both stages. It contains the extractant 5-nonylsalicylaldoxime and the diester 2,2,4-trimethyl-1,3-pentanediol diisobutyrate as a stripping modifier [131]. The structure of extractant in ACORGA M5640 is shown in **Figure 3.19**.

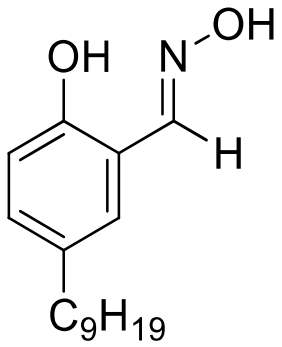

Figure 3.19- Structure of carrier (5-nonylsalicylaldoxime) in ACORGA M5640

The extraction process is summarized in Eq. 3.11. In extraction, the cation exchange extractants generate neutral complexes which are soluble in water immiscible solvents by interacting with the inner co-ordination sphere of the metal [123]. This demonstrates a so-called pH swing equilibrium mechanism, where a decrease in pH is observed upon metal complexation through the release of H^+ ions. H-bonds between the oximic H and phenolate O atoms provide an additional stability to the complex [182], [183] as shown in **Figure 3.20**. At low pH the oxime extractant is selective for copper, while other

metals such as nickel and zinc can be selectively recovered at higher pH. The loaded metal can then be efficiently stripped back upon contact with an excess inorganic acid as shown in Eq. 3.12 [123]. On treating with an excess acid, the release of metal ions into an aqueous solution and recovery of oxime ligand occurs due to the protonation of phenolate oxygen atoms [182]. The recovered oxime will be used again for the extraction of metal ions in another cycle.

$$\text{Extraction: } M^{2+}_{(aq)} + 2HL_{(org)} \rightleftharpoons M(L)_{2\,(org)} + 2H^{+}_{(aq)} \quad (3.11)$$

$$\text{Stripping: } M(L)_{2(org)} + 2H^{+}_{(aq)} \rightleftharpoons 2HL_{(org)} + M^{2+}_{(aq)} \quad (3.12)$$

Where M is copper or nickel

L is ligand in ACORGA M5640

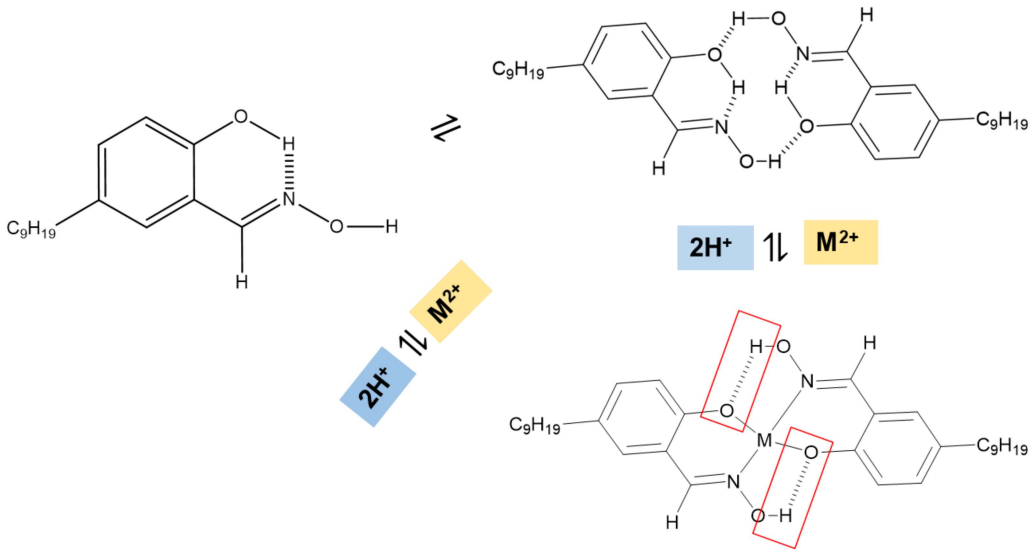

Figure 3.20- Summary of the process involved in the extraction of copper or nickel with ACORGA M5640

Parameters such as concentration of the extractant in organic phase, pH of the aqueous feed, extraction equilibrium time and organic to aqueous phase ratio were studied for the

effective transportation or extraction of metal into organic phase. Results are presented as a distribution coefficient (D) of a metal. It is defined as the ratio of concentration of metal in organic phase to that of metal in the aqueous phase at equilibrium as represented in Eq. 3.13 [184].

$$D = [M]_{org}/[M]_{aq.} \quad (3.13)$$

Where $[M]_{org}$ and $[M]_{aq}$ denotes the concentration of metal ions in the organic and aqueous phases at equilibrium, respectively.

From this, a separation factor (β) between two metals was also calculated as the ratio of distribution coefficient of two metals. For example, nickel over other metal such as cadmium or zinc can be defined as in Eq. 3.14.

$$\beta_{Ni/x} = D_{Ni}/D_x \quad (3.14)$$

where x represents the other metal.

Finally, the metal extraction can be presented as a simple percentage represented in Eq. 3.15.

% metal extraction = [M]org (post extraction)/[M]aq (pre extraction) * 100 (3.15)

where [M] denotes the concentration of metal

3.2.1. Solvent extraction of copper (SX1)

3.2.1.1. Effect of initial pH of the aqueous solution

As copper recovery using ACORGA M5640 is dependent on the initial pH of the aqueous solution[123], [185], the effect of pH of the nitric acid leach solution was studied between pH 1 and 3.5. Other parameters were: 30 °C temperature, 1:1 organic to aqueous phase ratio (O/A), 15 vol% ACORGA M5640 in kerosene and 60 min mixing time. Stirring

speed of 500 rpm was maintained in all experiments. It was found that the percentage extraction of copper into kerosene increased from 70 to 77% over pH 1 to 2.5, and then decreased from 77 to 54% over pH 2.5 to 3.5, leading to maximum extraction in the pH range 2 to 2.5 as shown **Figure 3.21**. The decrease in the extraction of copper at higher pH is due to the hydrolysis of copper ions [186]. Other metals such as zinc, lead and nickel were also poorly extracted (<10%) at pH 2.5. However, the concentration of these impurities in the organic solution was restricted to <5 mg/L. The distribution coefficients of copper, nickel, zinc and lead at different pH values, along with the separation factors of copper over nickel, zinc and lead are shown in **Table 3.2**. These results elucidate pH 2 is suitable for the maximum extraction of copper by minimizing the other impurities.

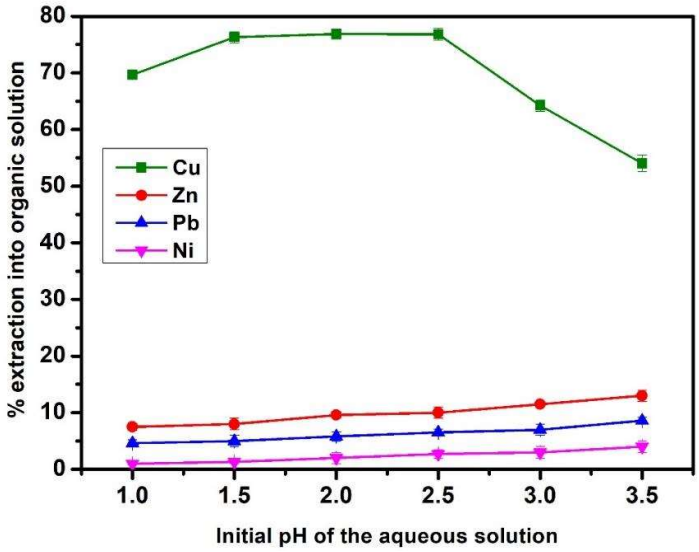

Figure 3.21- Effect of initial pH of the aqueous solution on the extraction of copper [Temp. 30 °C; time 60 min; org to aqueous phase ratio 1:1; concentration of oxime 15 vol% in kerosene]

Table 3.2- Distribution coefficient of copper, zinc, lead and nickel at different pH and separation factor of copper over zinc, lead and nickel [Temp 30 °C; time 60 min; org to aqueous phase ratio 1:1; concentration of oxime 15 vol% in kerosene]

pH	Distribution coefficient (D)				Separation Factor (β)		
	D_{Cu}	D_{Zn}	D_{Pb}	D_{Ni}	$\beta_{Cu/Zn}$	$\beta_{Cu/Pb}$	$\beta_{Cu/Ni}$
1	2.29	0.08	0.04	0.008	28.62	57.25	286.25
1.5	3.2	0.08	0.05	0.008	40	64	400
2	3.32	0.1	0.06	0.017	33.2	55.3	195.3
2.5	3.3	0.11	0.06	0.025	30	55	132
3	1.8	0.12	0.06	0.03	15	30	60
3.5	1.18	0.15	0.09	0.04	7.86	13.1	29.5

3.2.1.2. Effect of organic to aqueous phase ratio (O/A)

After optimization of pH, various organic to aqueous phase ratios were maintained such as 1:1, 1:1.5, 1:2, 1.5:1 and 2:1 at 30 °C, pH 2, 20 vol% of oxime concentration and 60 min mixing time to find out maximum transportation of copper. Results are shown in **Figure 3.22.** From the figure, it is evident that an increase in percentage extraction of copper across this range, reaching 93% at 1:1 ratio and maximizing at 99% for an O/A ratio of 2:1. The 1:1 O/A ratio was chosen as optimal in order to limit the volume of organic solvent. The transportation of zinc (11%), lead (8%) and nickel (4%) were also observed at 1:1 and their concentration was negligible (<5 mg/L) as compared to copper concentration (8400 mg/L). The resulting distribution coefficients and separation factors are reported in **Table 3.3**.

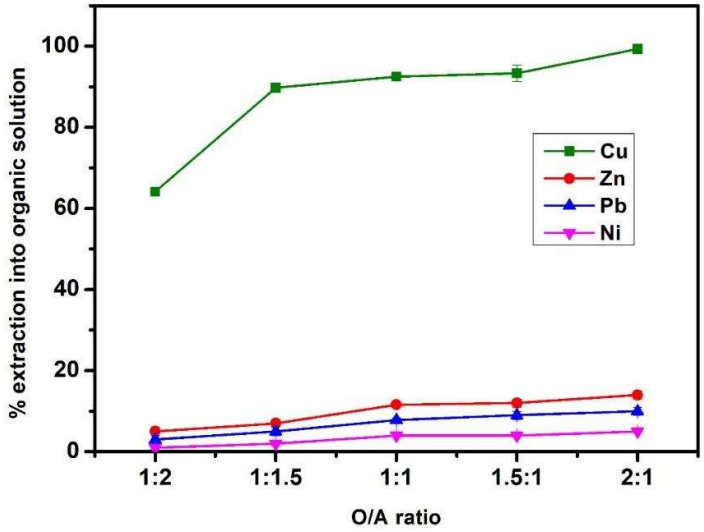

Figure 3.22- Effect of organic to aqueous phase ratio on extraction of copper [Temp. 30 °C; time 60 min; concentration of oxime 20 vol%; pH 2]

Table 3.3- Distribution coefficient of copper, zinc, lead and nickel at different organic to aqueous phase ratio and separation factor of copper over zinc, lead and nickel [Temp. 30 °C; time 60 min; concentration of oxime 20 vol%; pH 2]

O/A ratio	Distribution coefficient (D)				Separation Factor (β)		
	D_{Cu}	D_{Zn}	D_{Pb}	D_{Ni}	$\beta_{Cu/Zn}$	$\beta_{Cu/Pb}$	$\beta_{Cu/Ni}$
1:2	1.75	0.05	0.03	0.01	35	58.3	175
1:1.5	8.38	0.07	0.05	0.02	119.7	167.6	419
1:1	15.6	0.13	0.08	0.04	120	195	390
1.5:1	15.6	0.13	0.09	0.04	120	173.3	390
2:1	87	0.16	0.11	0.05	543.75	783.78	1740

3.2.1.3. Effect of concentration of extractant

The concentration of extractant ACORGA M5640 in kerosene was varied from 10 vol% to 30 vol% to study its effect on the extraction of copper. The remaining parameters were 1:1 O/A, pH 2, 30 °C temperature and 60 min mixing time. The transportation of copper into organic solution increased from 49.9 to 99.9% by increasing the concentration of ACORGA from 10 vol% to 30 vol%, as shown in **Figure 3.23**. In addition to that, zinc (11.6%), lead (7.8%) and nickel (4%) are also extracted into the organic solution at 30 vol% oxime. However, the concentrations of these impurities in the organic solution are less than 5 mg/L while copper concentration is 9080 mg/L. The distribution coefficients for the four metals at different concentrations of oxime, along with their respective separation factors are given in **Table 3.4.** Therefore, 30 vol% oxime in kerosene is optimized for the effective copper extraction.

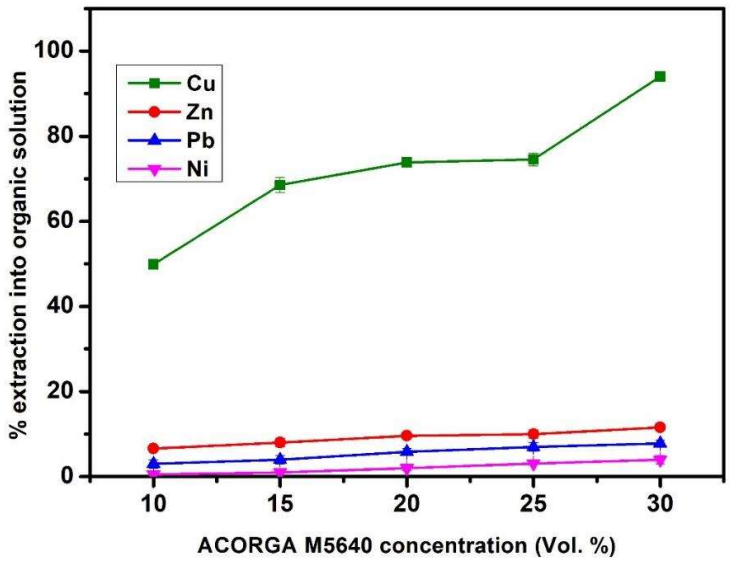

Figure 3.23- Effect of concentration of extractant on extraction of copper [Temp. 30 °C; time 60 min; O/A 1:1; pH 2]

Table 3.4- Distribution coefficient of copper, zinc, lead and nickel at different concentration of oxime (vol%) in kerosene and separation factor of copper over zinc, lead and nickel [Temp. 30 °C; time 60 min; O/A 1:1; pH 2]

Concentration of oxime (Vol.%)	Distribution coefficient (D)				Separation Factor (β)		
	D_{Cu}	D_{Zn}	D_{Pb}	D_{Ni}	$\beta_{Cu/Zn}$	$\beta_{Cu/Pb}$	$\beta_{Cu/Ni}$
10	1	0.07	0.03	0.005	14.29	33.33	200
15	2.17	0.08	0.04	0.01	27.12	54.25	217
20	2.82	0.1	0.06	0.02	28.2	47	141
25	2.91	0.11	0.07	0.03	26.45	41.57	97
30	87	0.16	0.11	0.05	543.75	783.78	1740

3.2.1.4. Effect of extraction equilibrium time

The mixing time of the solvent extraction was also varied from 20 to 80 min by keeping the other optimized parameters constant. As observed from **Figure 3.24**, 20 min of extraction equilibrium time was found to be sufficient for the maximum extraction of copper. Beyond this time, the percentage extraction was constant. The extraction of nickel, zinc and lead were also poorly extracted. The distribution coefficients and separation factors with respect to equilibrium contact time are given in **Table 3.5**.

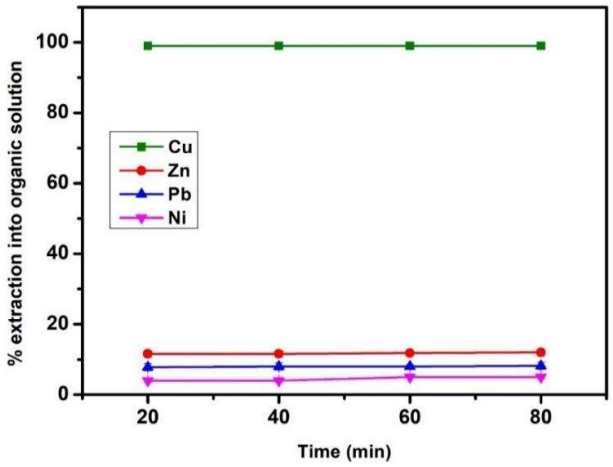

Figure 3.24- Effect of extraction equilibrium time on extraction of copper [Temp. 30 °C; concentration of oxime 30 vol%; O/A 1:1; pH 2]

Table 3.5- Distribution coefficient of copper, zinc, lead and nickel at different equilibrium time and separation factor of copper over zinc, lead and nickel [Temp. 30 °C; concentration of oxime 30 vol%; O/A 1:1; pH 2]

Extraction time (min)	**Distribution coefficient (D)**				**Separation Factor (β)**		
	D_{Cu}	D_{Zn}	D_{Pb}	D_{Ni}	$\beta_{Cu/Zn}$	$\beta_{Cu/Pb}$	$\beta_{Cu/Ni}$
20	87	0.13	0.08	0.04	669.2	1087	2175
40	87	0.13	0.08	0.04	669.2	1087	2175
60	87	0.16	0.11	0.05	543.7	790	1740
80	87	0.16	0.11	0.05	543.7	790	1740

Based on these experiments, the maximum transportation of copper (99.9%) into an organic phase in stage-1 solvent extraction process (SX1) was achieved by using 30 vol% ACORGA M5640 in kerosene, on a 1:1 organic to aqueous phase ratio held at pH 2, and with a contact time of 20 min. The individual elemental concentration of the feed solution, and resulting organic and raffinate solutions at these optimized conditions are shown in **Table 3.6**. It confirms the complete transport of copper, and traces of zinc, lead and nickel into the organic phase. Aqueous raffinate layer was separated and used for the selective recovery of nickel in stage-2 solvent extraction process. The organic solution was used for the back extraction of copper to produce pure copper solution.

Table 3.6- Variation of concentration of metals during SX1 of PCB leach solution [30 vol% ACORGA M5640 in kerosene; 20 min; 30 °C; O/A 1:1; pH 2]. Numbers in brackets shows error in mg/L [132]

Element	Concentration (mg/L)			Extraction (%)
	PCB stage-1 leach	SX1 Organic	SX1 raffinate	
Cu	9075(5)	9070(5)	5(1)	99.9
Ni	68(2)	3(1)	65(1)	4.4
Zn	43(1)	5(2)	38(2)	11.6
Pb	38(3)	3(1)	35(1)	7.8
Cd	43(2)	1(1)	40(2)	0
Ag	0.15(0.05)	0	0.1(0.05)	0
Sn	36(3)	2(1)	34(2)	0
Fe	0	0	0	0
Al	2(1)	0	2(1)	0

3.2.1.5. Effect of stripping reagent

Back extraction of copper from the organic phase into a fresh aqueous solution was the next important aspect to be investigated. As the metal-oxime complex formation operates under a pH swing mechanism (Eq. 3.12), adding an inorganic acid to the aqueous phase will increase the concentration of H^+ ions, thus pushing the equilibrium to the left to free the metal ions into the aqueous stripping phase. In this, the efficiency of copper recovery was observed by varying the stripping reagent (H_2SO_4 and HNO_3) at 30 °C, 1:1 organic to aqueous phase ratio for 60 min. It is found that 4 M sulfuric acid (pH −0.9) is more effective (92%) than 4 M HNO_3 (pH −0.6; 83%). But, these conditions also result in appreciable zinc and lead return. However, the overall concentrations of zinc and lead are low, at less than 5 mg/L and 3 mg/L respectively as shown in **Figure 3.25.** This results in a purified strip solution comprising 99.9% of the total copper content, along with minor

impurities of zinc (0.05%) and lead (0.02%). Recovery of elemental copper via electrowinning would be a well-established next step.

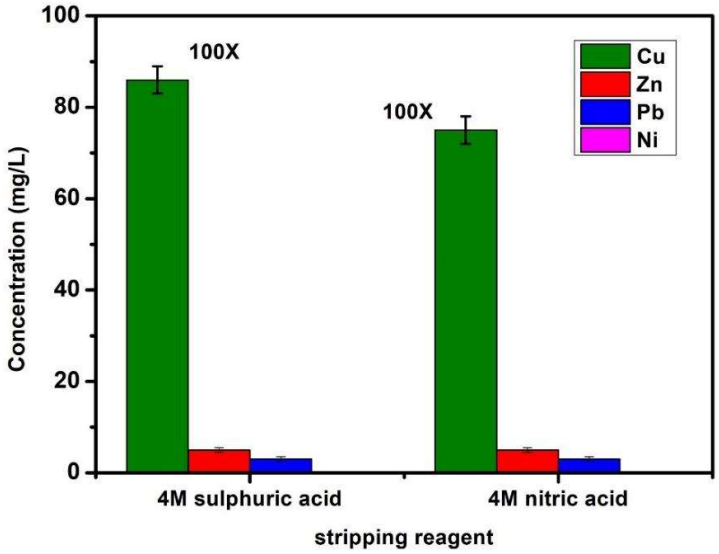

Figure 3.25- Effect of stripping reagent on the back extraction of copper [Temp. 30 °C; time 60 min; stirring speed 500 rpm; O/A 1:1]

3.2.2. Solvent extraction of nickel (SX2)

The elemental analysis of the raffinate solution following copper removal (SX1) indicated that the highest concentration of metals remaining were nickel (65 mg/L), cadmium (40 mg/L), tin (34 mg/L), lead (35 mg/L) and zinc (38 mg/L). All other metals are present at concentrations below 5 mg/L and therefore considered as trace impurities (**Table 3.6**). The performance of ACORGA M5640 to recover nickel was investigated while varying the pH of the aqueous solution, the concentration of the extractant in kerosene, the ratio of the aqueous and organic phases and the extraction equilibrium time. Results are presented as a distribution coefficient (D) and separation factor (β).

3.2.2.1. Effect of initial pH

The effect of varying the pH of the SX1 raffinate was investigated, with results presented in **Figure 3.26.** Other parameters were: 30 °C temperature, 1:1 organic to aqueous ratio (O/A), 30 vol% ACORGA M5640 in kerosene and 60 min mixing time. It was found that the percentage extraction of nickel gradually increased from 0 to 99.9% between pH 3 to 8, and then decreased. Above pH 8, nickel forms stable nickel-ammine complexes due to the presence of ammonia [187] which was added at the time of pH adjustment. Therefore, the decrease in the nickel extraction above pH 8 is observed [188]. Similar results using the LIX and ACORGA (i.e. maximum extraction at pH 8) were observed by Reddy et al., Mubarok et al., Sridhar et al., and Alguacil et al., [189]–[192]. Some zinc (maximum 42%, at pH 7) is co-extracted with nickel, but we note that the total concentration of zinc in the organic solution is low (14 mg/L). Cadmium ions were poorly extracted over this pH range. The distribution coefficients of nickel, zinc, cadmium at different pH values, along with the separation factors of nickel over zinc and cadmium are shown in **Table 3.7.** Based on these results, pH 8 was optimized for the effective transportation of nickel.

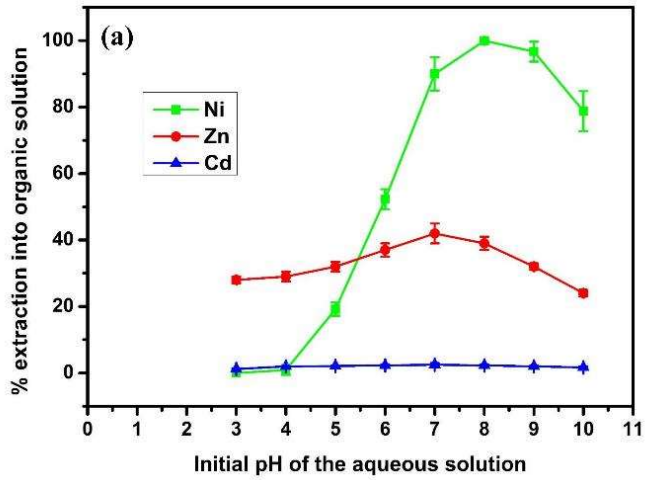

Figure 3.26- Effect of pH of aqueous solution on extraction of nickel [Temp. 30 °C; time 60 min; O/A ratio 1:1; concentration of oxime 30 vol%] [132]

Table 3.7- Distribution coefficient of nickel, zinc, cadmium at different pH and separation factors of nickel over zinc and cadmium [Temp. 30 °C; time 60 min; O/A 1:1; concentration of oxime 30 vol%] [132]

pH	Distribution coefficient (D)			Separation factor (β)	
	D_{Ni}	D_{Zn}	D_{Cd}	$\beta_{Ni/Zn}$	$\beta_{Ni/Cd}$
4	0.009	0.41	0.02	0.02	0.45
5	0.24	0.47	0.02	0.51	12
6	1.11	0.59	0.02	1.88	55
7	90	0.73	0.02	123	4500
8	32000	0.63	0.02	50793	1600000
9	30	0.47	0.02	64	1500
10	3.3	0.32	0.02	10	165

3.2.2.2. Effect of concentration of extractant

The extraction capacity of ACORGA M5640 for nickel was investigated by varying its concentration from 1 vol% to 35 vol% in kerosene at 30 °C, pH 8, O/A 1:1 for 60 min. Results in **Figure 3.27** show that the extraction of nickel increased from 87 to 99.9% with 1 to 10 vol% extractant in kerosene and then constant up to 35 vol%. Similarly, the extraction of zinc also increased with extractant concentration, but more slowly than observed for nickel. Based on this, an extractant concentration of 10 vol% is optimized for the effective separation of nickel over zinc. The low levels of cadmium recovered are essentially invariant to extractant concentration. The distribution coefficients for the three metals at different concentrations of oxime, along with their respective separation factors are given in **Table 3.8.**

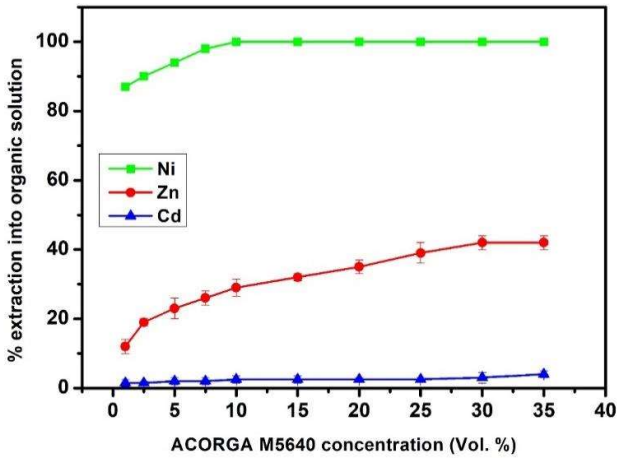

Figure 3.27- Effect of concentration of oxime on extraction of nickel [Temp. 30 °C; pH 8; time 60 min; O/A 1:1] [132]

Table 3.8- Distribution coefficient of nickel, zinc, cadmium at different concentration of oxime (vol%) in kerosene and separation factor of nickel over zinc and cadmium [Temp. 30 °C; time 60 min; O/A 1:1; pH 8] [132]

Concentration of oxime in kerosene (vol%)	**Distribution coefficient (D)**			**Separation factor (β)**	
	D_{Ni}	D_{Zn}	D_{Cd}	$\beta_{Ni/Zn}$	$\beta_{Ni/Cd}$
1	8.5	0.14	0.01	61	850
2.5	11.8	0.24	0.01	49	1180
5	13.6	0.3	0.02	45	680
7.5	56.2	0.35	0.02	160	2810
10	32000	0.42	0.02	76190	1600000

3.2.2.3. Effect of organic to aqueous phase ratio

The organic to aqueous phase (O/A) ratio is another variable that can affect the efficiency of the nickel recovery process. Various organic to aqueous phase ratios were maintained such as 1:50, 1:20, 1:10, 1:5, 1:2, 1:1.5, 1:1, 1.5:1 and 2:1 at 30 °C, pH 8, 10 vol% of ACORGA concentration and 60 min mixing time. From the result presented in **Figure 3.28,** it is clear that the extraction efficiency of nickel increases, maximizing (99.95%) at

1:5 and constant until 2:1. Therefore, O/A of 1:5 is optimized for the effective extraction of nickel. In addition, the extraction of zinc and nickel in the organic solution at 1:5 are minimized to 25% and 2% respectively. The resulting distribution coefficients and separation factors are reported in **Table 3.9.**

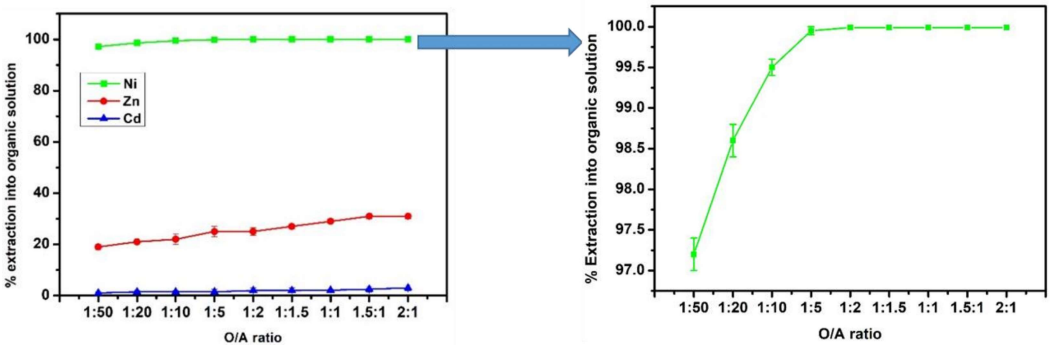

Figure 3.28- Effect of organic to aqueous phase (O/A) ratio on extraction of nickel [Temp. 30 °C; pH 8; concentration of oxime 10 vol%; time 60 min]

Table 3.9- Distribution coefficient of nickel, zinc, cadmium at different O/A phase ratio and separation factor of nickel over zinc and cadmium [Conditions: Temp. 30 °C; time 60 min; pH 8; concentration of oxime 10 vol%] [132]

O/A phase ratio	Distribution coefficient (D)			Separation factor (β)	
	D_{Ni}	D_{Zn}	D_{Cd}	$\beta_{Ni/Zn}$	$\beta_{Ni/Cd}$
1:50	36	0.24	0.01	150	3600
1:20	72	0.27	0.01	266	7200
1:10	213	0.3	0.01	710	21300
1:5	38730	0.33	0.01	117360	3873000
1:2	38730	0.33	0.02	117360	1936500
1:1.5	38730	0.4	0.02	96825	1936500
1:1	38730	0.425	0.02	91130	1936500
1.5:1	38730	0.46	0.02	84196	1936500
2:1	38730	0.46	0.02	84196	1936500

3.2.2.4. Effect of extraction equilibrium time

Finally, the extraction equilibrium time was also investigated for maximum transportation of nickel at the optimized parameters, with results shown in **Figure 3.29.** While almost all (99.7%) of the nickel is observed within 15 minutes, traces of nickel ions (0.1 mg/l) are still observed in the raffinate until 45 min. Therefore, an equilibrium time of 60 minutes likely represents the optimum time needed for complete formation of the nickel oxime complex in the organic phase on a single contact process. Re-contacting the raffinate with a recycled extractant layer regenerated following the strip phase would likely increase the percentage of metal recovered allowing shorter contact times [123]. The distribution coefficients and separation factors with respect to equilibrium contact time are given in **Table 3.10.**

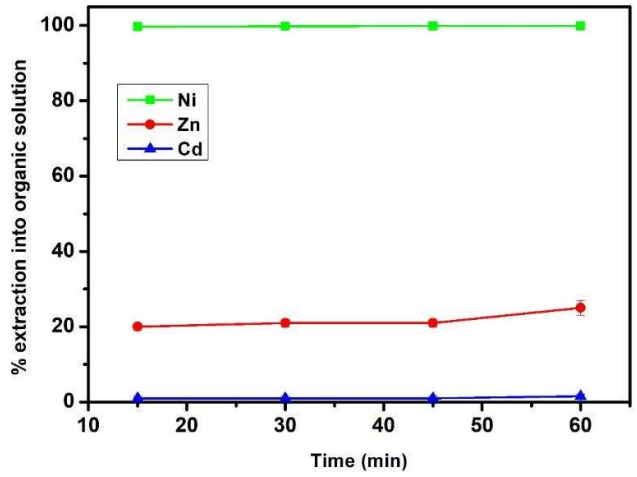

Figure 3.29- Effect of equilibrium time on extraction of nickel from the post-copper leach solution [Temp. 30 °C; pH 8; concentration of oxime 10 vol%; O/A 1:5] [132]

Table 3.10- Distribution coefficient of nickel, zinc, cadmium at different equilibrium time and separation factor of nickel over zinc and cadmium [Temp. 30 °C; pH 8; O/A 1;5; concentration of oxime 10 vol%] [132]

Time (min)	Distribution coefficient (D)			Separation factor (β)	
	D_{Ni}	D_{Zn}	D_{Cd}	$\beta_{Ni/Zn}$	$\beta_{Ni/Cd}$
15	389	0.26	0.01	1496	38900
30	516	0.26	0.01	1985	51600
45	25800	0.29	0.01	88965	2580000
60	39030	0.32	0.01	121968	3903000

Based on these experiments, the maximum transportation of nickel into an organic phase in a single SX contact is achieved by using 10 vol% ACORGA M5640 in kerosene, on a 1:5 organic to aqueous phase ratio held at pH 8, and with a contact time of 60 min. The individual elemental concentration of the SX2 feed solution, and resulting organic and raffinate solutions at these optimized conditions are shown in **Table 3.11**. It confirms that near complete transport of nickel, and partial transport of low levels of zinc (9 mg/L) and cadmium (0.8 mg/L), all other trace elements remain in the aqueous raffinate layer.

Table 3.11- Variation of concentration of metals (mg/L) during stage 2 solvent extraction, SX2 [pH 8; 10 vol% ACORGA M5640 in kerosene; 60 min; 30 °C; O/A 1:5]. Numbers in brackets represent error in mg/L [132]

Element	Concentration (mg/L)			Extraction (%)
	SX1 raffinate	SX2 organic	SX2 raffinate	
Cu	5(1)	0	5(1)	0
Ni	65(1)	64(1)	0.01	99.7
Zn	38(2)	9(1)	28(1)	25
Pb	35(1)	0	31(1)	0
Cd	40(2)	0.8(1)	39(1)	2
Ag	0.1(0.05)	0	0.1	0
Fe	0	0	0	0
Al	2(1)	0	2(1)	0

3.2.2.5. Effect of stripping reagent

Back extraction of the nickel from the organic phase into a fresh aqueous solution was also investigated at 30 °C, organic to aqueous ratio 1:1 for 60 min. Here, the efficiency of nickel recovery was assessed by varying the concentration (0.1-1.0 M) of three different acid stripping reagents (H_2SO_4, HCl and HNO_3), with results presented in **Figures 3.30**. It is found that all acids acted as efficient stripping agents, indicating a certain flexibility in the system that could be exploited to encourage a good material balance for the overall process. From the data presented in Figure 3.30, maximum nickel recovery was shown by stripping using 0.5 M HCl (pH −0.9) or 1.0 M nitric acid (pH ~0), which showed 96% nickel recovery. However, these conditions also result in appreciable zinc and cadmium return (22% and 62%, respectively). However, it is worth noting, that the overall concentrations of zinc and cadmium are low, at less than 2 mg/L and 0.6 mg/L respectively as shown in **Figure 3.31** and **Figure 3.32.** The optimized extraction and stripping parameters result in a purified strip solution comprising 97.2

wt% of the total nickel content, along with minor impurities of zinc (2.7 wt%) and cadmium (< 0.1wt%).

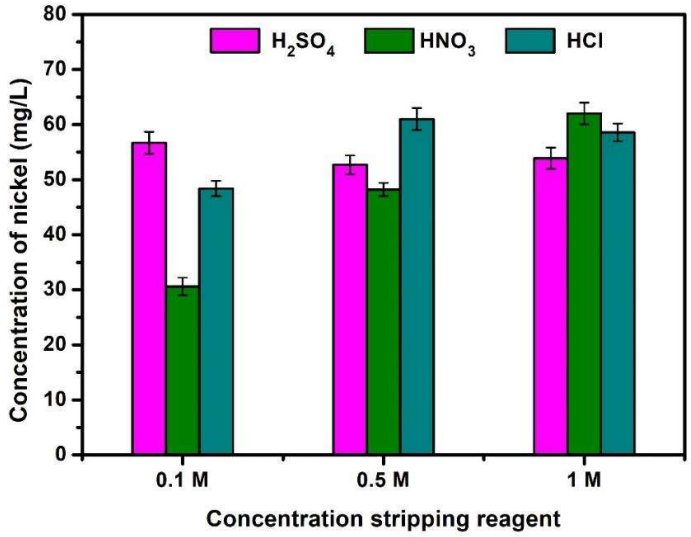

Figure 3.30- Effect of stripping reagent on the back extraction of nickel [Temp. 30 °C; time 60 min; O/A 1:1]

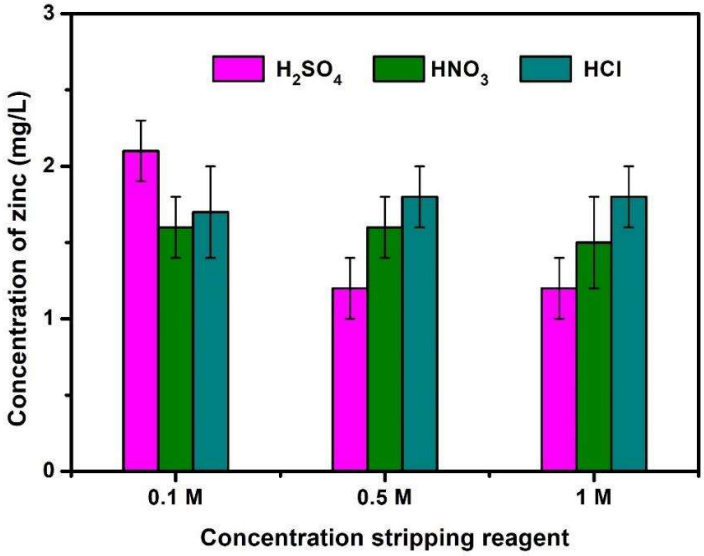

Figure 3.31- Effect of stripping reagent on the back extraction of zinc [Temp. 30 °C; time 60 min; O/A 1:1]

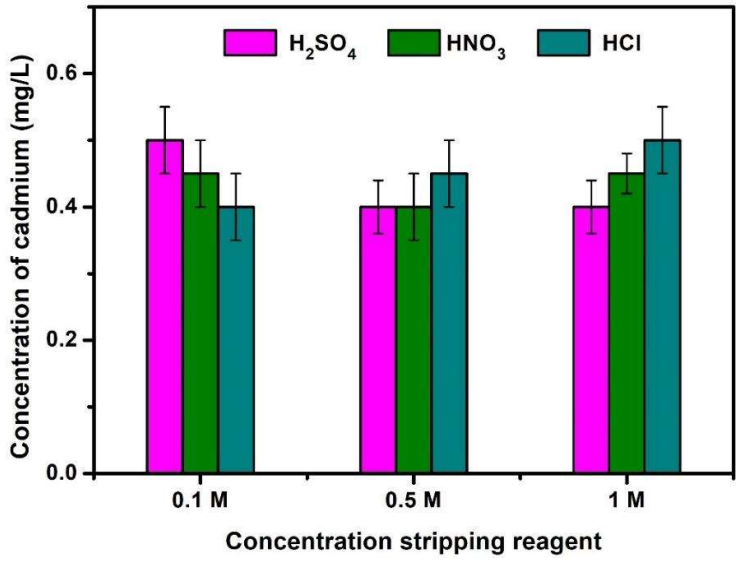

Figure 3.32- Effect of stripping reagent on the back extraction of cadmium [Temp. 30 °C; time 60 min; O/A 1:1]

Recovery of elemental nickel via electro winning would be a well-established next step. To study the efficacy of the separated organic solvent, it was used for another extraction cycle under the same optimized conditions. Upon recycling the extractant layer up to five times, extraction levels of nickel on the order of 99% were still be obtained from a fresh leach liquor.

3.2.3. Separation of trace elements from SX2 raffinate by cementation

As zinc is also one of the minor elements in the SX2 raffinate, the addition of zinc minimizes the risk of introducing other chemical species and produces pure zinc solution by the precipitation of copper, cadmium, lead and tin. The addition of zinc powder (74 µm) at 50 °C temperature with 500 rpm stirring speed was used. An excess amount (300% excess) of zinc powder than the stoichiometric requirement was utilized to overcome its dissolution due to the reduction of H^+ ions during cementation. It was observed that the concentration of lead, tin, copper and cadmium was dropped down to ~0 mg/L in 60 min

(Figure 3.33) while the concentration of zinc was increased to 103 (7) mg/L. The pH of the solution was increased from 3 to 8 due to the reduction of H^+ ions [193], [194]. After 1 hour of cementation, the trace elements were precipitated out and pure zinc nitrate solution was also separated from the precipitate through filtration. The reduction of zinc by electrowinning, or the utilization of zinc nitrate solution for catalytic applications, the synthesis of nanocomposites is the future scope of the work to improve the economic viability. The spent electrolyte could also be used again in the leaching process.

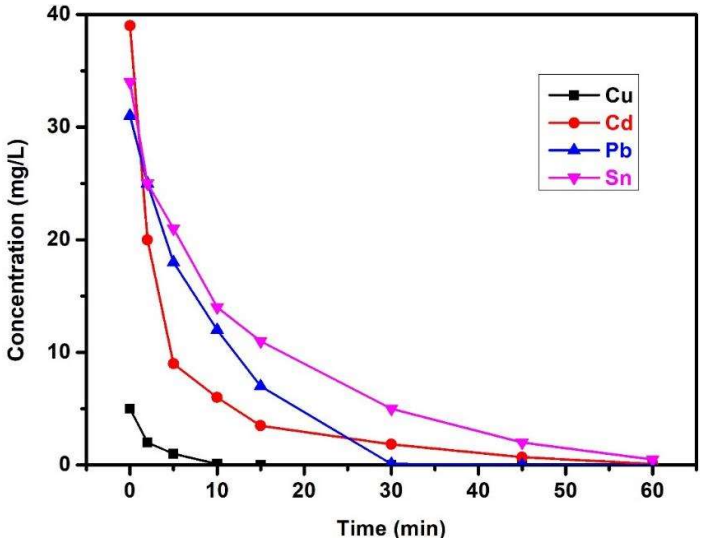

Figure 3.33- Cementation of minor elements (Cu, Cd, Pb, and Sn) on zinc powder from SX2 raffinate [Temp. 50 °C; time. 60 min; stirring speed 500 rpm; amount of zinc powder 300% excess; size of zinc powder 74 μm] [132]

The filtered residue was analyzed with the X-ray diffraction analysis. XRD pattern of the precipitate is shown in **Figure 3.34**. It displays the presence of lead nitrate, lead, copper oxide, cadmium, dicopper (nitrate (v)) trihydroxide, oxides of tin and zinc and nitrammite in the residue. The increase in pH during cementation and the presence of ammonia in the solution corroborated the formation of nitrate complexes in the precipitate [195].

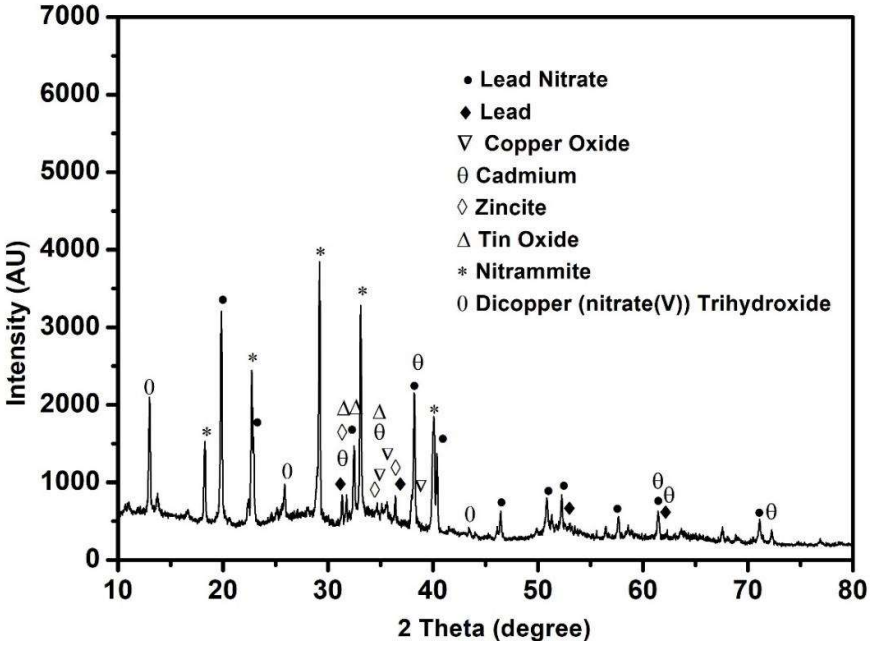

Figure 3.34- XRD analysis of filtered residue [132]

The sequential recovery of copper and nickel through two-stage solvent extraction process and separation of other traces through cementation from SX2 raffinate is expected to ensure economic and industrial feasibility.

Conclusions

This study has shown that the use of the industrial extractant ACORGA M5640 is efficient for the sequential recovery of copper and nickel from a base leach liquor of waste mobile phone PCBs through two-stage solvent extraction. The various important points relevant to the present sections are listed below.

- Solvent extraction of copper (SX1) with oxime is pH dependent, with maximum extraction (99.9%) observed at pH 2, 1:1 organic to aqueous phase ratio with 30 vol% oxime concentration in 60 min by leaving nickel rich raffinate solution.
- Traces of zinc, lead and nickel were also co-extracted into the organic phase.

- The extracted copper ions are readily stripped from the extractant, with more than 92% recovered, along with low levels of zinc (5 mg/L) and lead (3 mg/L) with 4 M sulfuric acid.
- The purity of the final strip solution contained 99.92 wt% copper, along with 0.047 wt% zinc and 0.023 wt% lead.
- In stage 2 solvent extraction (SX2), quantitative extraction of nickel (99.9%) is achieved using a 1:5 organic (10 vol% extractant in kerosene) to aqueous (pH 8) phase ratio in 60 min.
- Low levels of zinc (9 mg/L) and cadmium (0.8 mg/L) are also co-extracted into the organic phase.
- The nickel is readily stripped from the extractant, with more than 95% recovered, along with low levels of zinc (1.7 mg/L) and cadmium (0.02 mg/L), following a 0.5 M hydrochloric acid or 1 M nitric acid strip step.
- The purity of the final strip solution contained 97.2 wt% nickel, along with 2.7 wt% zinc and < 0.1 wt% cadmium.
- The extraction efficiency of a recycled extractant layer after 5 cycles performed to a similar standard as a fresh organic solution, with a slight volume loss attributed to phase separation.
- The separation of traces from SX2 raffinate reveals that the removal of copper, lead, tin and cadmium; and the generation of pure zinc solution is obtained by adding 300% excess zinc powder (74 μm) at 50 °C with 500 rpm stirring speed in 60 min.
- The separation of copper in stage 1, nickel from copper-free aqueous solution in stage 2 and other minor elements from the raffinate of stage 2 solvent extraction ensures the

proposed process is sustainable and avoids complexity in the sequential metal recovery processes.

Section-3

Separation of gold and silver from stage-2 leach solution

3.3. Separation of gold and silver from stage-2 leach solution

This chapter explains about the selective recovery of gold and silver from the second stage leach solution of mobile phone PCBs. The process of generation of stage-2 leach solution was explained in detail in **section 3.1.** The recovery of Au(III) was observed using solvent extraction with an organic amide diluted in toluene as an extractant by leaving other elements in the raffinate. The separation of silver from raffinate was also examined by the chemical precipitation (cementation) with copper powder.

3.3.1. Separation of gold from stage-2 leach solution by solvent extraction

The protonation of an amide plays a crucial role in the selective extraction of Au(III) into the organic phase. Combination of the protonated and neutral amide with $[AuBr_4]^-$ through hydrogen bonding and electrostatic interactions creates a neutral assembly and transport into the organic phase. The process of Au(III) extraction with primary amide as an extractant diluted in toluene is shown in **Figure 3.35**. Back extraction of $[AuBr_4]^-$ from the amide neutral complex into an aqueous phase is also essential for the generation of pure gold solution and the re-generation of free extractant for another extraction cycle. The process of back extraction or striping with either water or sodium hydroxide is also shown in **Figure 3.36.**

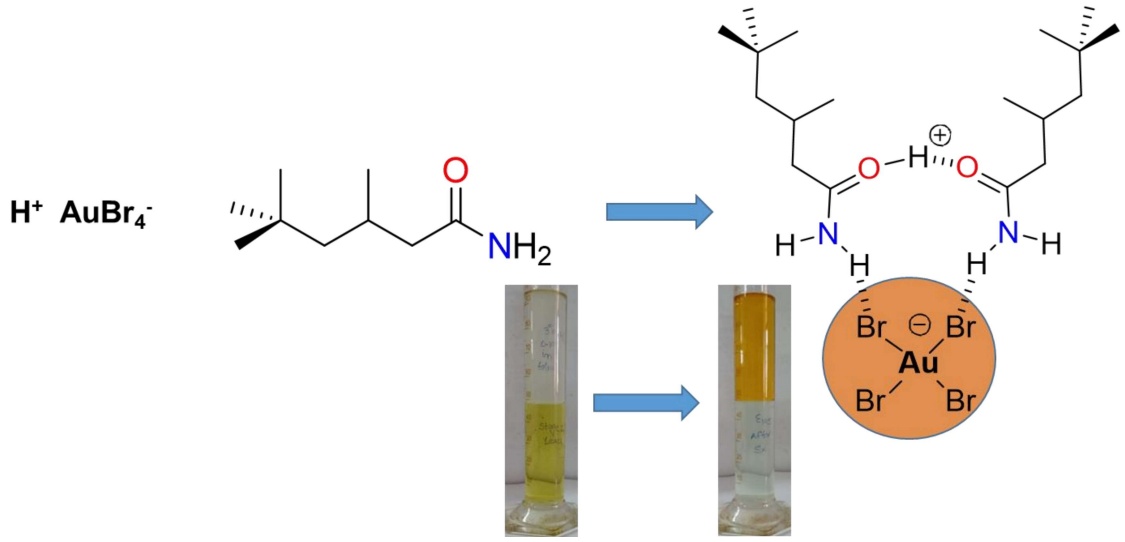

Figure 3.35- Summary of the process involved in the extraction of Au(III) from an aqueous leach solution into an organic phase containing primary amide

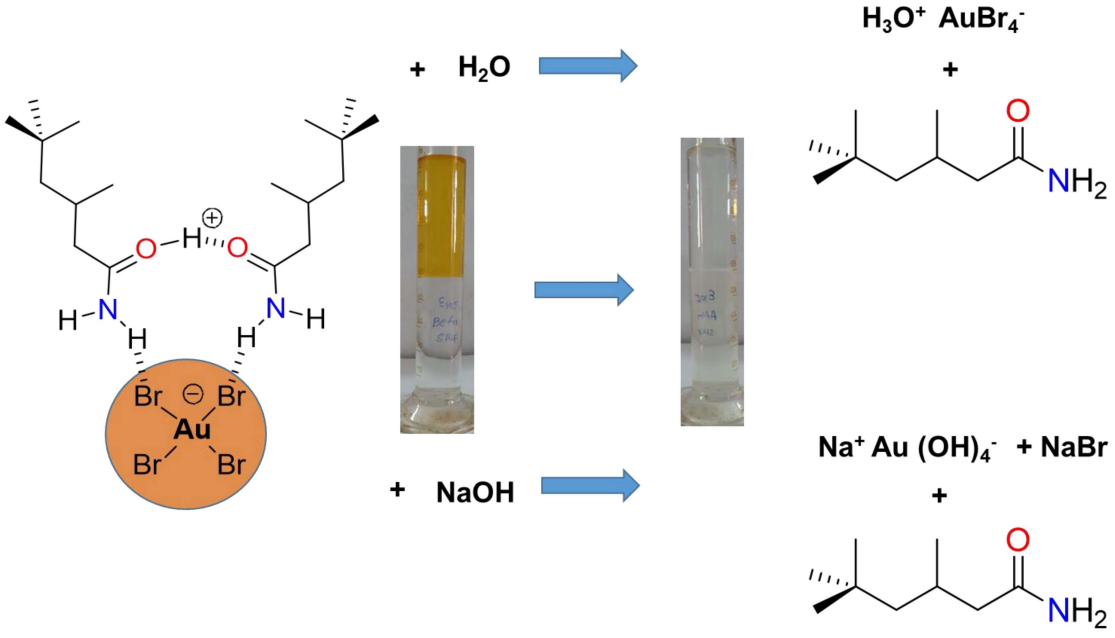

Figure 3.36- Summary of the process involved in the back extraction of Au(III) from primary amide complex into an aqueous (water or sodium hydroxide) solution

3.3.1.1. Effect of type of amide on gold extraction

Stage-2 leach solution consists of gold (8.8 mg/L), silver (20 mg/L), tin (120 mg/L) and traces of copper (10 mg/L). The transportation of gold from the leach liquor into a toluene solution of either 0.1 M primary (**1°, L^1**), secondary (**2°, L^2**) or tertiary amide (**3°, L^3**) as extractants was evaluated individually. Other parameters were: 20 °C temperature, 1:1 organic to aqueous phase ratio (O/A), 500 rpm stirring speed and 60 min mixing time. The results are presented in **Figure 3.37.**

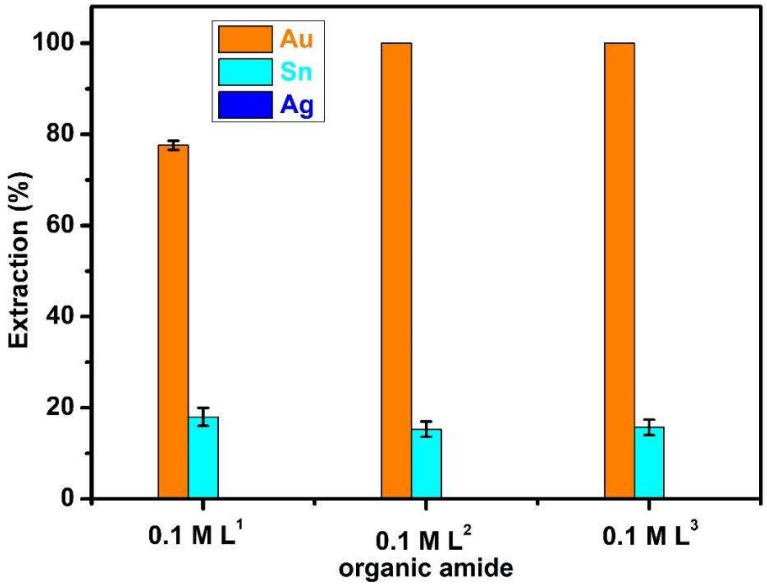

Figure 3.37- Extraction of metals from the stage-2 leach liquor by a toluene solution of 0.1 M primary (**L^1**), secondary (**L^2**), or tertiary amide (**L^3**) [O/A 1:1; time: 60 min; temp. 20 °C; stirring speed 500 rpm] [112]

From the figure, it is evident that the amount of gold extracted into the organic phase increased from **L^1** (78%) to **L^2** (99.9%) and **L^3** (99.9%). In addition to gold, a proportion of tin (15-18%) is also extracted by all amides. However, no silver is seen. The

distribution coefficients of gold and tin with **L[1], L[2]** and **L[3]** along with the separation factor of gold over tin are shown in **Table 3.12.**

Table 3.12- Distribution coefficient of gold and tin at different types of amides and separation factor of gold over tin

Type of amide	Distribution coefficient (D)		Separation factor (β)
	D_{Au}	D_{Sn}	$\beta_{Au/Sn}$
L[1]	3.5	0.2	17.5
L[2]	1130	0.17	6647
L[3]	1130	0.17	6647

These analyses indicate that stronger gold extraction occurs with the secondary and tertiary amides **L[2]** and **L[3]** compared with the primary amide **L[1]**. Unlike in previous work [137], no third phases were seen during the extractions which is likely due to the relatively simple mixture of metals present in the second-phase leach solution compared with the multi-metal leach solution previously investigated.

3.3.1.2. Effect of stripping reagent

The stripping of the individual metals from the metal-loaded toluene solution was evaluated using water and two concentrations of sodium hydroxide (0.1 and 1 M). Other parameters were: 20 °C temperature, 1:1 organic to aqueous phase ratio, 500 rpm stirring speed and 60 min mixing time. The results are shown in **Figure 3.38.** While no gold is stripped into water from metal-loaded toluene solutions of **L[1]** and **L[2]**, 11.5% of gold is stripped with water from extraction solutions of **L[3]**. Using 0.1 M NaOH solution as the stripping reagent, increases gold stripping for **L[1]** (40%), **L[2]** (78%) and **L[3]** (82.6%). Almost all gold recovery is only achieved from all amide extractions when 1 M NaOH is used as the stripping reagent. Therefore, 1 M sodium hydroxide was chosen for the back

extraction of gold from either secondary or tertiary amides. The need for a NaOH stripping solution may be a consequence of the use of bromide in this process instead of chloride, for which water stripping was seen to be effective [136].

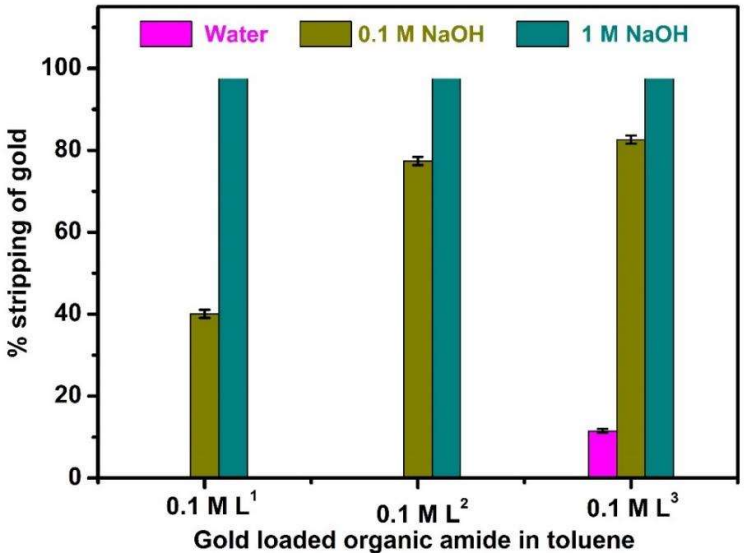

Figure 3.38- Effect of reagent on stripping of gold from the organic phase, using 0.1 M $\mathbf{L^{1-3}}$ in toluene as the extracting reagent [O/A 1:1; time: 60 min; temp. 20 ^{o}C; stirring speed 600 rpm] [112]

In addition to gold, tin is also stripped from the amide extraction solutions to some extent, and gradually decreases from $\mathbf{L^1}$ to $\mathbf{L^3}$ with all stripping reagents as shown in **Figure 3.39.** The figure shows that traces of tin (10%) were only found with 1 M sodium hydroxide as a stripping reagent from tertiary amide.

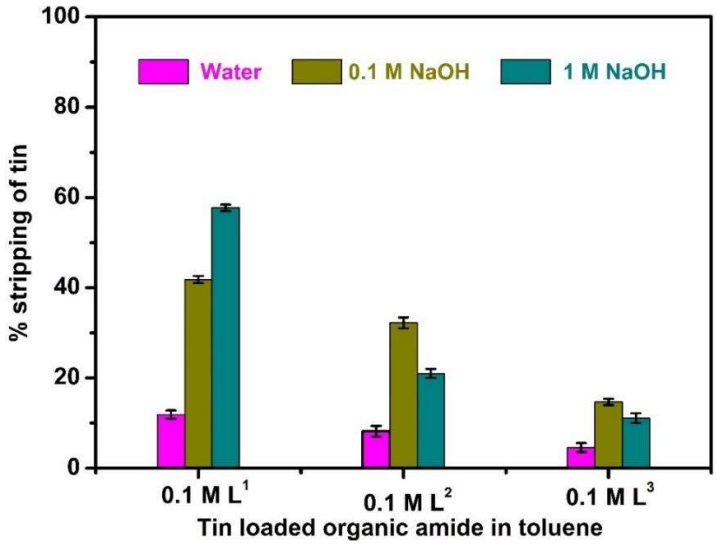

Figure 3.39- Effect of reagent on stripping of tin from the organic phase, using 0.1 M $\mathbf{L^{1-3}}$ in toluene as the extracting reagent [O/A 1:1; time 60 min; temp. 20 ^{o}C] [112]

Based on these results, quantitative separation of gold (99.9%) by solvent extraction of the stage-2 leach solution is achieved using 0.1 M of $\mathbf{L^3}$ as the carrier agent in toluene, followed by stripping with 1 M sodium hydroxide. Chemical analysis of the strip solution revealed that it consists of 8.8 mg/L gold along with 1.98 mg/L tin. After another cycle of extraction and stripping, the strip solution comprises 8.8 mg/L gold with 0.03 mg/L tin. Further purification of gold from tin could potentially be achieved through additional extraction and strip cycles. The produced gold solutions could be subjected to standard reduction processes for the isolation of metallic gold or could be used to synthesize nanoparticles or catalysts to potentially increase the economic value [196]–[199].

3.3.2. Separation of silver from raffinate through Cementation

The elemental analysis of the raffinate solution following gold removal indicated that the presence of metals remaining were tin (47 mg/L), silver (10 mg/L) and copper (5 mg/L). As copper is also one of the minor elements in the solution, the addition of copper minimizes the risk of introducing other chemical species and precipitates silver by

cementation by leaving tin behind. Different parameters such as quantity of copper powder, temperature and stirring speed were optimized for attaining efficient silver recovery.

3.3.2.1. Optimization of the quantity of copper powder

In order to separate silver from the solution, the quantity of copper required was optimized initially. For that, copper powder (325 mesh) with different quantities such as 30 mg, 100mg, 200mg and 300 mg in 100mL solution were used at 30 °C with 500 rpm stirring speed. The percentage cementation of silver and change in the concentration of tin and copper while separation of silver from the solution with different dosages of copper powder are shown in **Figure 3.40.**

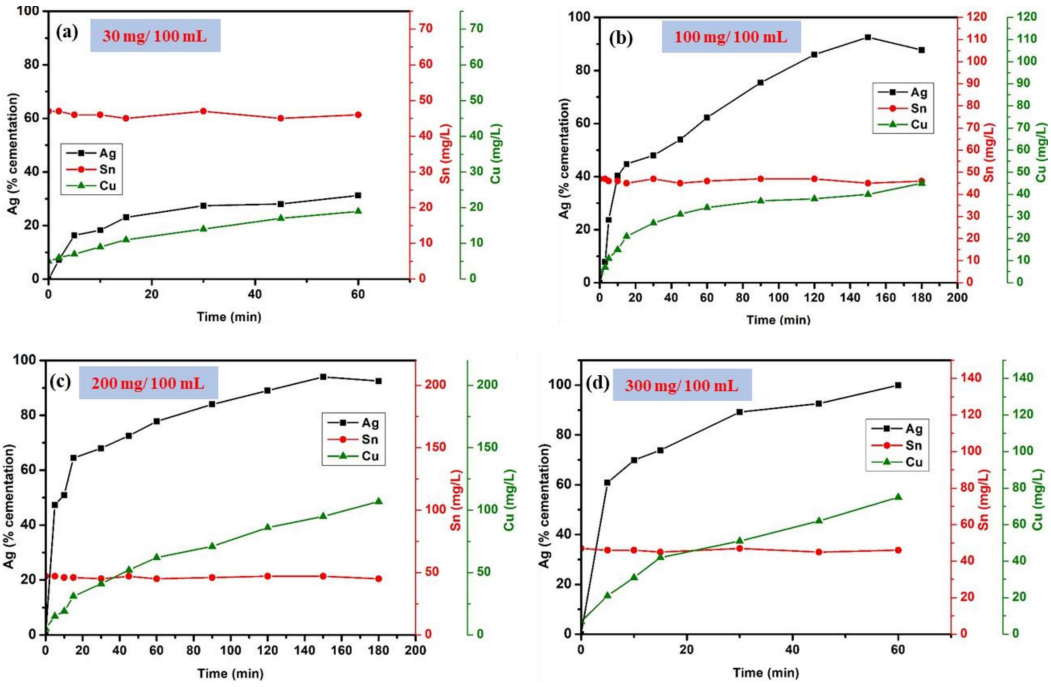

Figure 3.40- Effect of quantity of copper powder on cementation of silver (a) 30 mg/100mL (b) 100 mg/100 mL (c) 200 mg/100mL (d) 300 mg/100 mL [Temp. 30 °C; stirring speed 500 rpm; size of dust 325 mesh]

It can be seen from figure that the cementation yield is too slow with 30 mg as it reaches 31% in 60 min. Whereas, with 100 mg and 200 mg, the cementation percentage gradually increases to 92% and 94% respectively in 150 min and then decreases due to the re-dissolution of silver. Because, as more residue is precipitated, it tends to re-dissolve again under the action of oxygen present in the solution [200]. The effective cementation of silver was observed within 60 min with 300 mg copper powder. A significant increase in copper concentration is also observed in all cases due to its dissolution. However, the concentration of tin was not changed in all cases and it was constant (47 mg/L) throughout the process. Based on these observations, 300 mg copper powder with 60 min is optimized as the most suitable quantity for the separation of silver from the solution.

3.3.2.2. Effect of temperature

Four experiments were conducted at different temperatures from 30 to 60 °C, fixing the total time of cementation at 60 min. Other parameters were: 300 mg/100 mL copper powder (325 mesh) and 500 rpm stirring speed. The results are shown in **Figure 3.41**. From these investigations, it was observed that the cementation of silver reaches 99% in all cases (from 30 to 60 °C) albeit the reduction in residence time with increasing temperature. The concentration of copper is also increased at higher temperatures, i.e. from 40 to 60 °C. Lower temperature (30 °C) is optimized to reduce excess copper dissolution and high-energy consumption.

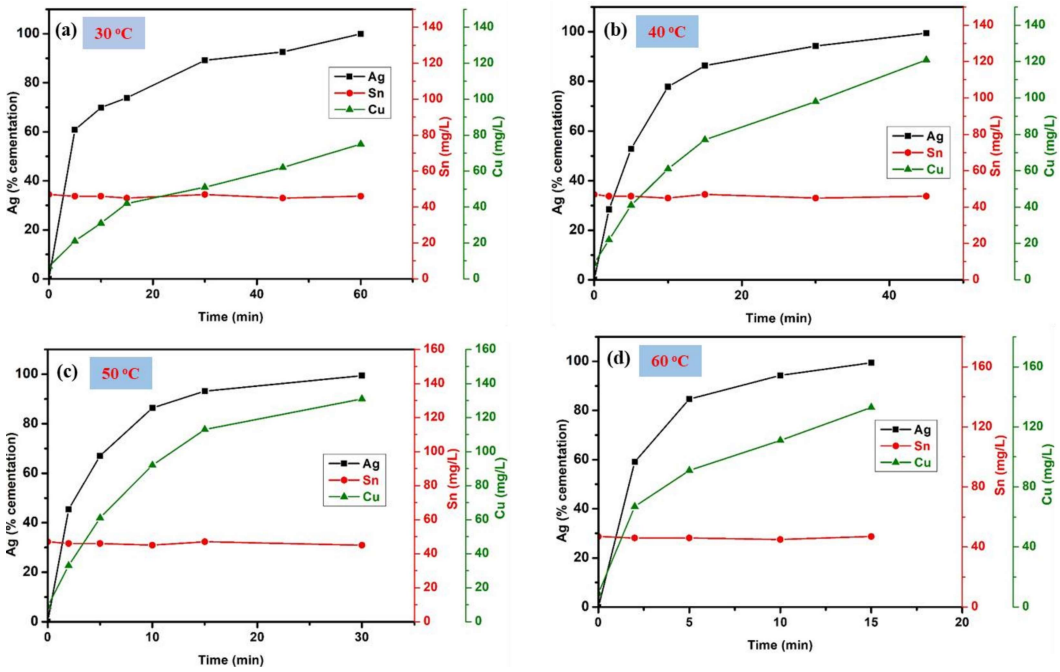

Figure 3.41- Effect of temperature on cementation of silver (a) 30 °C (b) 40 °C (c) 50 °C (d) 60 °C [quantity of copper powder 300 mg/100mL; stirring speed 500 rpm; size of dust 325 mesh]

3.3.2.3. Effect of stirring speed

Finally, the stirring speed was varied between 100 and 500 rpm using 300 mg/100ml copper powder at 30 °C temperature for 60 min. The experiments show that the cementation yield of silver increases slightly with increasing stirring speed and reaches 99.99% silver cementation yield at 500 rpm as shown in **Figure 3.42.** In addition, the dissolution of copper is similar in all cases and the concentration of tin was not changed. Therefore, 500 rpm stirring speed was selected as the optimal value.

Based on these studies, the quantitative cementation of silver was observed at 30 °C, 500 rpm with 300 mg/100 mL solution.

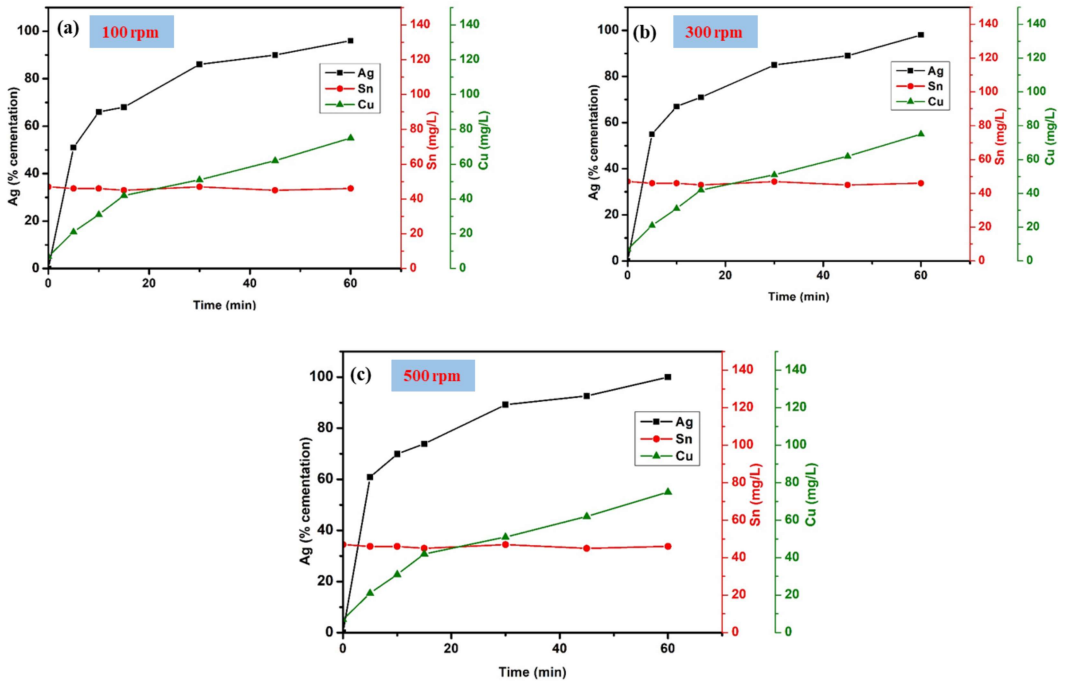

Figure 3.42- Effect of stirring speed on cementation of silver (a) 100 rpm (b) 300 rpm (c) 500 rpm [Temp. 30 °C; quantity of copper powder 300 mg/100mL; size of dust 325 mesh]

3.3.2.4. Analysis of Residue

During cementation, the dissolved silver reacted with copper and precipitated out. After filtration, the residue was collected, washed, dried and analyzed in SEM-EDS to check its composition. SEM-EDS of the filtered residue is shown in **Figure 3.43.** It displays the presence of precipitated silver fraction along with copper in the residue.

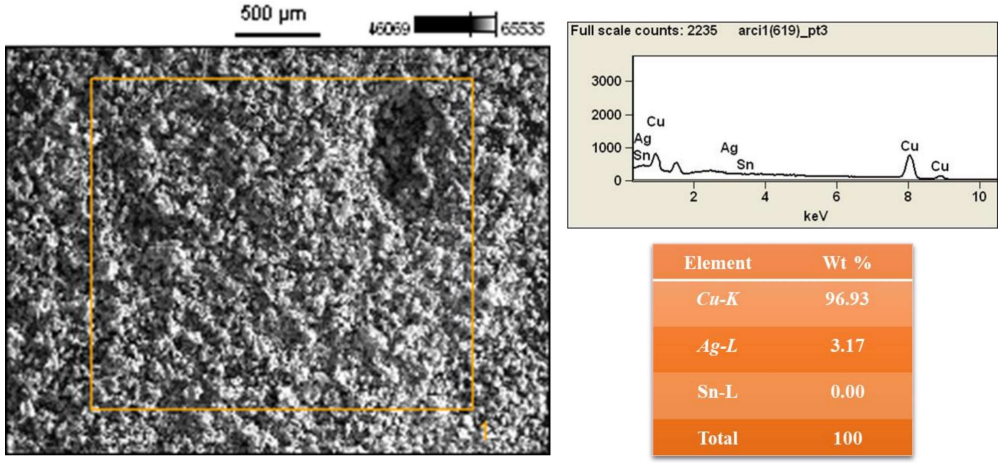

Figure 3.43- SEM-EDS analysis of filtered residue

3.3.2.5. Kinetics of cementation

The cementation of silver with copper occurs according to Eq. 3.16.

$$2Ag^{+} + Cu \rightarrow 2Ag + Cu^{2+} \qquad (3.16)$$

It is reported that the cementation reactions mostly follow first-order kinetics [201], [202]; we also assumed first-order kinetics for silver cementation and plots were linearly fitted according to Eq. 3.17. BET surface area analysis revealed the surface area of copper powder is 50.5×10^{-2} m^2/g. **Figure 3.44 (a)** represents the graphs between $-\ln (C_{Ag\,t}/C_{Ag\,i})$ vs time at various temperatures and the rate constant of the reaction is also calculated with the help of the slope of the linear plots.

$$-\ln (C_{Ag\,t}/C_{ag\,i}) = k(A/V)t \qquad (3.17)$$

where k= Rate constant

A= Surface area of copper powder

V= Volume of the solution

$C_{Ag\,t}$ = Concentration of silver at time t

$C_{ag\,i}$ = Initial silver concentration

t = Time (min)

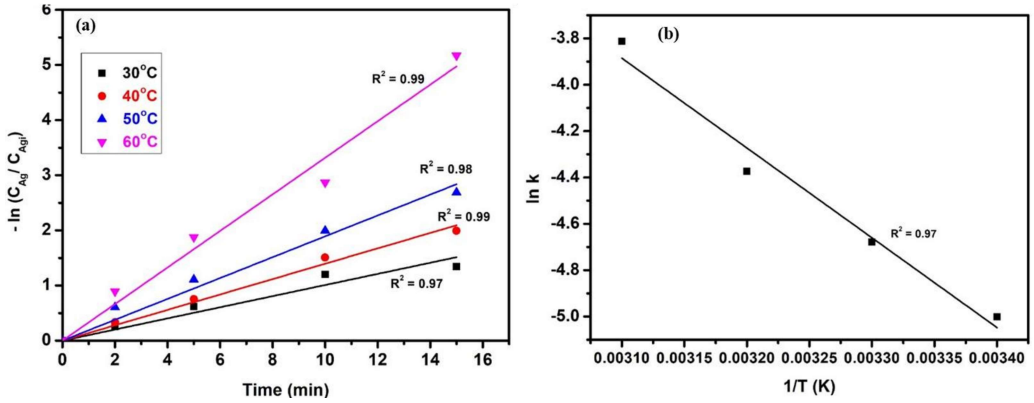

Figure 3.44- (a) First order kinetics and (b) corresponding Arrhenius plots for the cementation of silver

Finally, the experimental activation energy was calculated for the cementation of silver with the help of a linearly fitted Arrhenius plot (ln k vs 1/T), which was also shown in the **Figure 3.44 (b).**

Slope of the Arrhenius plot= $-E_a/R$= (-3873.75)

Where E_a = Activation energy

R = Gas constant

The obtained activation energy for the cementation is calculated as 32.2 kJ/mole.

Conclusions

- The use of 0.1 M tertiary (**L^3**) amide is efficient for the transportation of Au(III) into toluene solution at 1:1 organic to aqueous phase ratio at 20 °C by leaving silver, tin and traces of copper in the raffinate.
- Tin was also co-extracted along with gold.
- The extracted Au(III) was stripped from the toluene solution, with 99.9% recovered, with 1M NaOH as stripping reagent.
- The purity of the final strip solution contained 8.8 mg/L gold and 0.03 mg/L tin after two extraction cycles.
- Chemical precipitation (cementation) of silver was also observed from the raffinate of gold solvent extraction stage.
- 300 mg/100 mL copper powder was effective for 99.9% cementation of silver at 30 ^{o}C with 500 rpm stirring speed.
- SEM-EDS analysis confirmed the presence of silver in the precipitate along with copper.

Section- 4

Validation of two-stage leaching through Response Surface Methodology (RSM) - A DOE study

3.4. Validation of two-stage leaching through Response Surface Methodology (RSM) - A DOE study

Design of experiments (DOE) is an effective tool that can be used in various experimental situations by reducing the number of experiments to optimize an effective response and save time [203]. Response surface methodology (RSM) is a DOE modelling technique used to assess the relative importance of parameter variation by coupling the quantitative data obtained from experiments to mathematical and statistical equations to facilitate the parameter optimization process [204]. Herein, a three-factor, three-coded level (low: -1, centred: 0, and high: +1) central composite design (CCD) based RSM was used to validate the optimal conditions for the two-stage leaching. For stage-1 leaching validation, time (A), concentration of nitric acid (B) and stirring speed (C) were considered as independent variables (factors), with copper and nickel leaching considered as response variables. Similarly, time (A), temperature (B) and stirring speed (C) were considered as independent variables (factors), with gold leaching as the response variable for stage-2 leaching. The whole process provides the effect of individual and combined parameters on response variables, an analysis of mathematical models for the process optimization, and a check on the adequacy of the model. The representation of lower and higher levels of independent variables is shown in **Table 3.12** and **Table 3.13** by assuming the optimized value is in between them based on the experimental optimization. CCD with three parameters forms a cube representing corner points, axial and centre points, as shown in **Figure 3.45.**

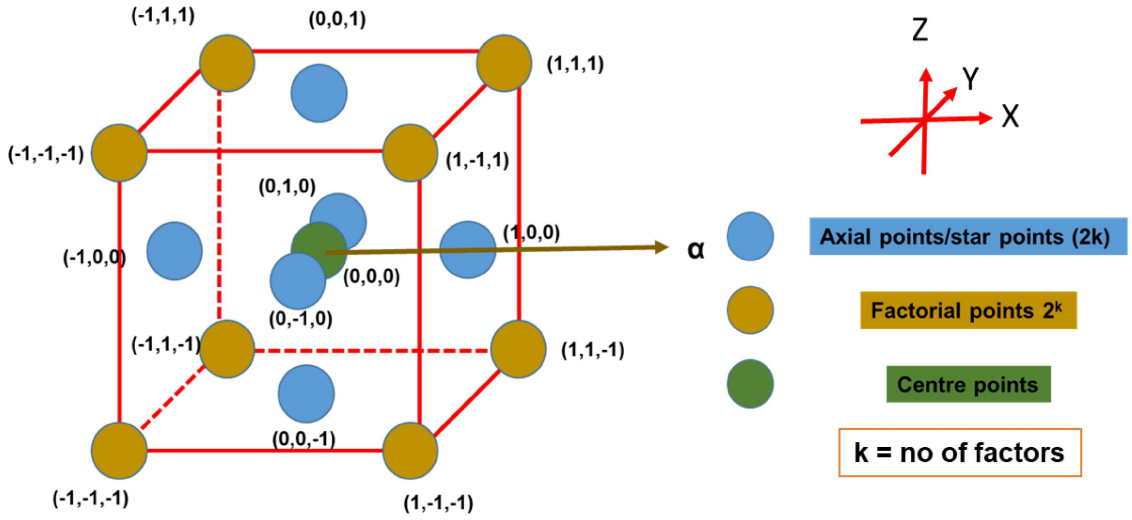

Figure 3.45- Generation of Central Composite Design (CCD) for three factors

Alpha (α) is the distance of each axial point (a point lies on any of the axes of a coordinate system) from the centre in a central composite design. An alpha value less than one (<1) puts the axial points in the cube; a value equal to one (=1) puts them on the faces of the cube, and a value greater than one (>1) puts them outside the cube. Here in this work, alpha is chosen as 1 and the axial points lie on the faces of the cube. Therefore, minus alpha and plus alpha values are also equal to the lower and higher levels of the factors in **Table 3.13 and Table 3.14.**

Table 3.13- RSM parameters for copper and nickel leaching [169]

Name of the factor	Units	Low (-1)	High (+1)	-alpha	+alpha
Time (A)	min	5	120	5	120
Conc. of nitric acid (B)	M	1	3	1	3
Stirring speed (C)	rpm	100	500	100	500

Table 3.14- RSM parameters for gold leaching

Name of the factor	Units	Low (-1)	High (+1)	-alpha	+alpha
Time (A)	min	10	60	10	60
Temperature (B)	°C	30	90	1	3
Stirring speed (C)	rpm	100	500	100	500

The optimal parameter conditions for selective metal leaching through two-stage leaching was described in **section 3.1**, and approximated by considering each variable in isolation. A more in-depth analysis of the variables can be obtained by analyzing the data by RSM. Thus, this section explains the validation of optimized two-stage leaching parameters with the RSM of DOE.

3.4.1. Validation of stage-1 leaching by response surface methodology

To this end, the different factors or parameters with different levels for optimization were input into Design-Expert 13 software. This created 17 different conditions of experimental runs by taking factorial points (six), corner points (eight) and a centre point (with a repetition of three times). From this, the effect of individual and combined factors on response could be gauged. Each experimental run except the centre point run (#7, #12 and #17) was repeated in triplicate, and the average response value and standard deviation (error) are recorded in **Table 3.15**. Similarly, Run #7 was repeated in triplicate with the repeats logged as run #12 and #17. Three levels of factors were taken by keeping temperature (30 °C) and pulp density (50 g/L) variable constant. The response values i.e. leaching percentage was varied from 0 to 99.9%. The lowest leaching of copper and nickel was observed when two of the three factors were at their lowest level, while the highest leaching was seen at the highest level of at least two of them.

Table 3.15- Central composite design table for the leaching of copper and nickel [169]

	Factor 1	Factor 2	Factor 3	Response 1	Error (%)	Response 2	Error (%)
Run	**A:Time (min)**	**B:Conc. of nitric acid (M)**	**C:Stirring speed (rpm)**	**copper leaching (%)**		**nickel leaching (%)**	
1	120	3	100	94.2	1.2	98	1
2	120	1	100	39	2	51.7	1
3	62.5	1	300	34	1	26.2	1.2
4	5	1	500	0	0	0	0
5	5	3	500	1	0	6.6	0.6
6	120	3	500	99.9	0	99.9	0
7	62.5	2	300	55.5	-	38.8	-
8	5	2	300	0.6	0	0	0
9	120	1	500	43	1	54.8	0.8
10	5	3	100	0.8	0.2	1	0
11	62.5	2	100	54	1	37.3	1.3
12	62.5	2	300	57	-	39.8	-
13	62.5	2	500	59.3	1.3	41	1
14	5	1	100	0.4	0	0	0
15	120	2	300	79	2	78	1
16	62.5	3	300	68.6	1.6	55	2
17	62.5	2	300	58.5	-	40.8	-

The individual responses for copper and nickel leaching from the above table were fitted and analyzed using quadratic and two-factor interaction (2FI) models. Based on these analyses, the leaching of copper and nickel can be expressed mathematically in terms of the coded variables shown in Eq. 3.18 and Eq. 3.19. The accuracy or adequacy of fit of the regression model for the above equations was analyzed using analysis of variance (ANOVA) (**Tables 3.16 and 3.18**). ANOVA explains the effect of single factors and

interactions of the factors on the model. The impacts of time (<0.0001 p-value) and concentration of nitric acid (<0.0001 p-value) were greater than stirring speed as their probability (p) values are very low. It also contains the sum of squares, degrees of freedom (df), mean square, model significant (F) value. The greater the F value above the unity and lower p values show the significance of the model. The low p values ($p < 0.001$) and higher F values of the regression model and the observation of non-significant lack of fits in both cases show that they are statistically significant [3], with R^2 values of 0.9965 and 0.9985 (**Tables 3.17 and 3.19**). Reasonable agreement between adjusted R^2 and predicted R^2 within 0.2 of each other was also observed.

$$\text{Cu leaching (coded)} = 56.76 + 35.24\,A + 14.82\,B + 1.49\,C + 13.85\,AB + 1.25\,AC + 0.3\,BC - 16.79\,A^2 - 5.29\,B^2 + 0.0641\,C^2 \quad (3.18)$$

$$\text{Ni leaching (coded)} = 39.35 + 37.49\,A + 12.79\,B + 1.44\,C + 10.49\,AB - 0.0638\,AC + 0.5637\,BC \quad (3.19)$$

where A= time

B= concentration of nitric acid, and

C= stirring speed.

Table 3.16- ANOVA quadratic model for copper leaching [169]

Source	Sum of Squares	df	Mean Square	F-value	p-value	
Model	17829.99	9	1981.11	220.13	< 0.0001	significant
A-Time	12418.58	1	12418.58	1379.91	< 0.0001	
B-Conc. of nitric acid	2196.32	1	2196.32	244.05	< 0.0001	
C-Stirring speed	22.20	1	22.20	2.47	0.1603	
AB	1534.58	1	1534.58	170.52	< 0.0001	
AC	12.50	1	12.50	1.39	0.2771	
BC	0.7200	1	0.7200	0.0800	0.7855	
A^2	754.92	1	754.92	83.88	< 0.0001	
B^2	74.86	1	74.86	8.32	0.0235	
C^2	0.0110	1	0.0110	0.0012	0.9731	
Residual	63.00	7	9.00			
Lack of Fit	58.50	5	11.70	5.20	0.1691	not significant
Pure Error	4.50	2	2.25			
Corrected Total	17892.98	16				

The model F-value of 220.13 with <0.001 p-value implies the model is significant. P-values less than 0.05 also indicate model terms are significant. The lack of fit F-value of 5.20 implies that the lack of fit is not significant relative to the pure error. Non-significant lack of fit is usually desirable.

Table 3.17- Fit statistics for copper leaching [169]

Std. Dev.	**3.00**	***R²***	**0.9965**
Mean	43.82	Adjusted R^2	0.9920
C.V. %	6.85	Predicted R^2	0.9729
		Adeq Precision	44.8620

Table 3.18- ANOVA two factor interaction (2FI) model for nickel leaching [169]

Source	**Sum of Squares**	**df**	**Mean Square**	**F-value**	**p-value**	
Model	16594.10	6	2765.68	1099.39	< 0.0001	significant
A-Time	14054.25	1	14054.25	5586.70	< 0.0001	
B-Conc. of nitric acid	1636.10	1	1636.10	650.36	< 0.0001	
C-Stirring speed	20.65	1	20.65	8.21	0.0168	
AB	880.53	1	880.53	350.02	< 0.0001	
AC	0.0325	1	0.0325	0.0129	0.9117	
BC	2.54	1	2.54	1.01	0.3384	
Residual	25.16	10	2.52			
Lack of Fit	23.16	8	2.89	2.89	0.2821	not significant
Pure Error	2.00	2	1.0000			
Corrected Total	16619.26	16				

The model F-value of 1099.39 with <0.0001 p-value implies the model is significant. The lack of fit F-value of 2.89 implies that the lack of fit is not significant relative to the pure error. The higher R^2 values also signify a higher correlation between the observed and predicted values [205] as shown in **Figure 3.46**.

Table 3.19- Fit statistics of nickel leaching [169]

Std. Dev.	**1.59**	***R²***	**0.9985**
Mean	39.35	Adjusted R^2	0.9976
C.V. %	4.03	Predicted R^2	0.9910
		Adeq Precision	101.6278

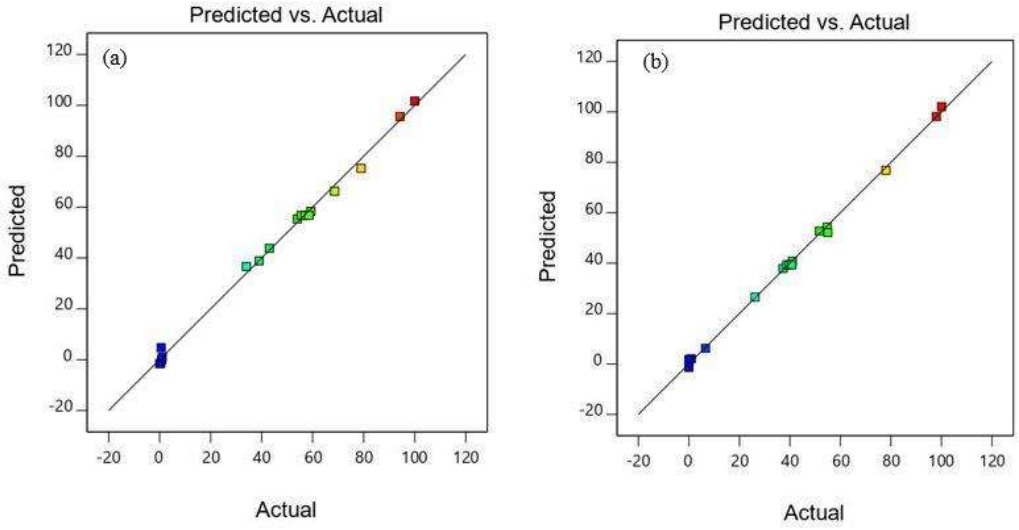

Figure 3.46- Predicted vs actual plots for (a) copper and (b) nickel leaching

Finally, in order to gain better understanding of interaction effects of variables on the leaching of copper and nickel, 3-dimensional response surface plots and 2-dimensional contour plots were drawn as shown in **Figure 3.47 and Figure 3.48**. These show that the leaching efficiency of copper and nickel at a fixed stirring speed (500 rpm) increases with increasing the residence time and the concentration of nitric acid. Similarly, at a constant concentration of nitric acid (3 M), the leaching efficiency increases with increased residence time, and stirring speed. Blue colour indicates the lowest leaching and red colour indicates the highest leaching in figures.

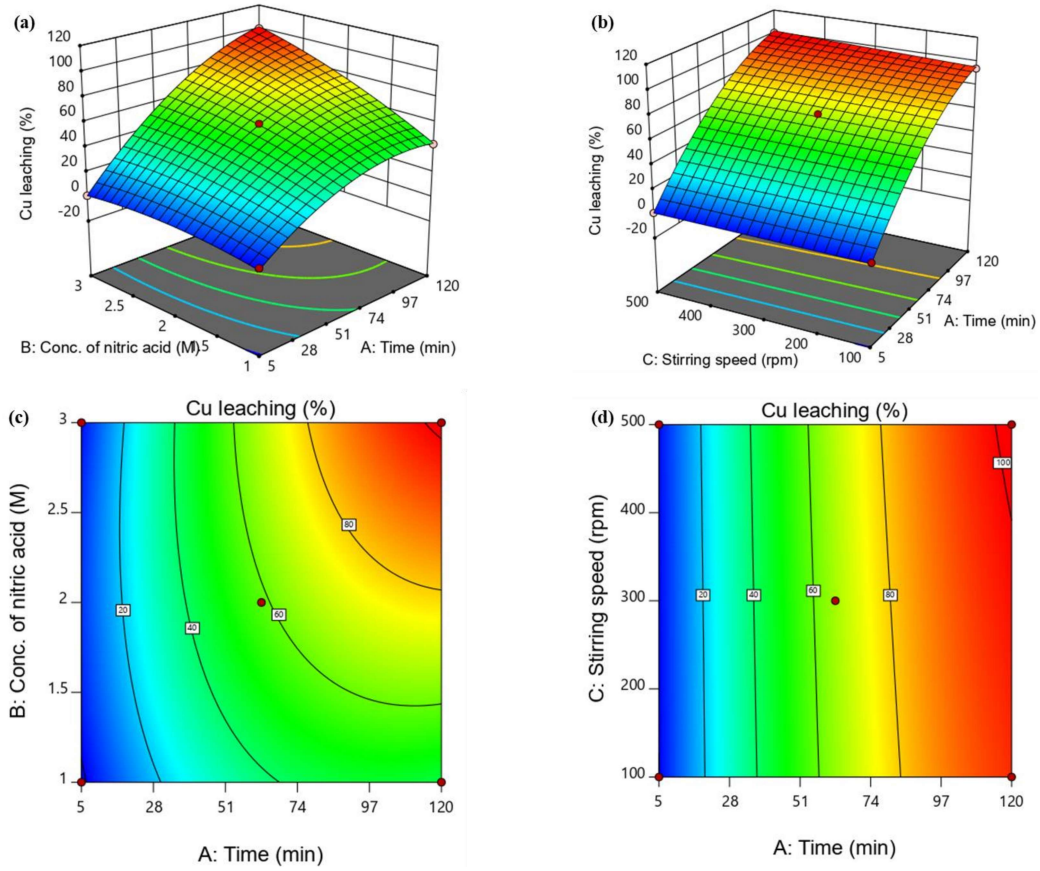

Figure 3.47- Three-dimensional response surface plots and two-dimensional contour plots for the leaching of copper [(a) and (c) represents at a constant stirring speed of 500 rpm, (b) and (d) represents at constant concentration of nitric acid of 3 M]

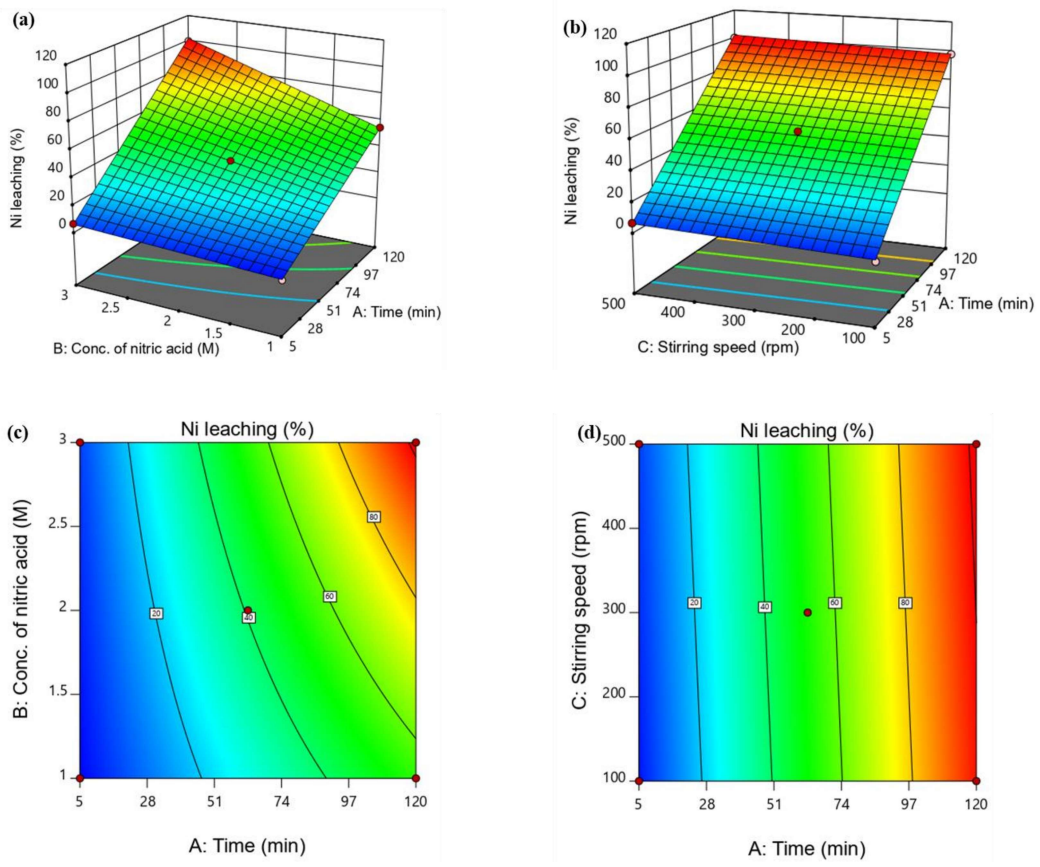

Figure 3.48- Three-dimensional response surface plots and two-dimensional contour plots for the leaching of nickel [(a) and (c) represents at a constant stirring speed of 500 rpm, (b) and (d) represents at constant concentration of nitric acid of 3 M]

The RSM optimization of parameters show that the quantitative leaching of copper and nickel occurs at 120 min, using 2.92 M nitric acid, and at 490 rpm stirring speed as presented in **Figure 3.49**.

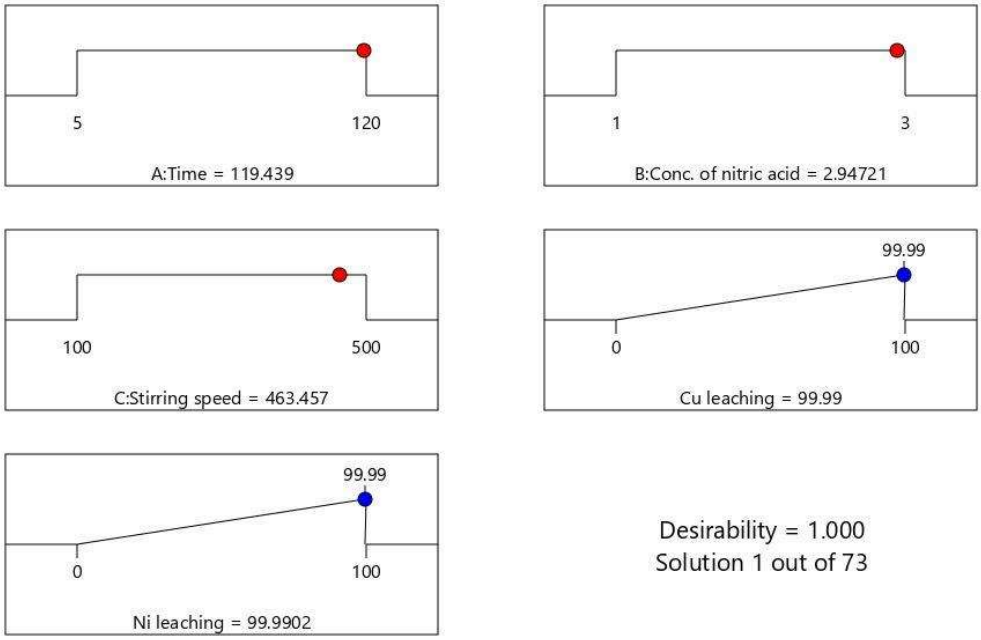

Figure 3.49- Optimization of parameters for the leaching of copper and nickel

Comparing these data with the experimental optimizations, showed a similar effect on copper and nickel leaching in the mentioned range of parameters. Thus, the DOE approach has validated the experimental data and interpretation put forward in **section 3.1**, and clearly establishes that optimal conditions have been met without the need for further classical experimental optimization.

3.4.2. Validation of stage-2 leaching by response surface methodology

For the validation of gold leaching, 20 different conditions of experimental runs were created by taking factorial points (six), corner points (eight) and centre points (with a repetition of six times) to increase the adequacy of the model. These experiments were conducted by taking lower, centred and higher values of the factors, from which the effect of individual and combined variables or factors could be determined. Each experimental run except centre point was repeated in triplicate, and the average response value and

standard deviation (error) are recorded in **Table 3.20**. Similarly, the centre point was repeated six times and tabulated the response value. Three levels of factors were varied with 3 M sulfuric acid with 3M sodium bromide as a leaching reagent.

Table 3.20- Central composite design table for the leaching of gold

	Factor 1	Factor 2	Factor 3	Response 1	Error (%)
Run	**A:Time**	**B:Temp**	**C:Stirring speed**	**gold leaching**	
	min	°C	rpm	%	
1	35	60	500	87	1
2	35	60	300	85	-
3	10	90	100	73	1
4	35	60	300	84	-
5	60	90	100	86	1
6	60	90	500	88	0
7	35	60	300	84	-
8	10	90	500	75	0
9	35	60	300	85	-
10	35	60	100	83	0
11	35	90	300	84	0
12	35	60	300	86	-
13	10	30	500	68	1
14	35	30	300	75	0
15	10	60	300	73	1
16	60	30	500	82	2
17	60	30	100	80	1
18	10	30	100	66	1
19	60	60	300	89	2
20	35	60	300	85	-

The individual responses for gold leaching from the above table were fitted and analyzed by the higher-order and significant quadratic model. Based on this analysis, the leaching

of gold can be expressed mathematically in terms of the coded variables shown in Eq. 3.20. The accuracy or adequacy of fit of the regression model for the above equations was analyzed using analysis of variance (ANOVA) (**Tables 3.21**). ANOVA explains the effect of time (<0.0001 p-value) and temperature (<0.0001 p-value) were greater impacts than stirring speed (0.0039 p-value). The low p values ($p < 0.001$) and higher F values of the regression model and the observation of non-significant lack of fit show that they are statistically significant. Higher correlation values with predicted R^2 of 0.933 and adjusted R^2 of 0.9776 is in reasonable agreement with difference <0.2 were also observed as shown in table **Tables 3.22**. The representation of predicted vs actual R2 values are shown in **Figure 3.50.**

$$\text{Au leaching (coded)} = 84.63 + 7.00\,A + 3.50\,B + 1.20\,C - 0.25\,AB - 3.32\,A^2 - 4.82\,B^2 + 0.\ 0.6818\,C^2 \quad (3.20)$$

Table 3.21- ANOVA quadratic model for gold leaching

Source	Sum of Squares	df	Mean Square	F-value	p-value	
Model	863.49	9	95.94	93.07	< 0.0001	significant
A-Time	490.00	1	490.00	475.31	< 0.0001	
B-Temp	122.50	1	122.50	118.83	< 0.0001	
C-Stirring speed	14.40	1	14.40	13.97	0.0039	
AB	0.5000	1	0.5000	0.4850	0.5020	
AC	0.0000	1	0.0000	0.0000	1.0000	
BC	0.0000	1	0.0000	0.0000	1.0000	
A^2	30.28	1	30.28	29.37	0.0003	
B^2	63.84	1	63.84	61.93	< 0.0001	
C^2	1.28	1	1.28	1.24	0.2915	
Residual	10.31	10	1.03			
Lack of Fit	7.48	5	1.50	2.64	0.1553	not significant
Pure Error	2.83	5	0.5667			
Cor Total	873.80	19				

The model F-value of 93.07 with a p-value <0.0001 implies the model is significant. P-values less than 0.0500 indicate model terms are significant. In this case A, B, C, A^2, B^2 are significant model terms. Values greater than 0.1000 indicate the model terms are not significant. The lack of fit F-value of 2.64 implies the lack of fit is not significant relative to the pure error.

Table 3.22- Fit statistics for gold leaching

Std. Dev.	1.02	R^2	0.9882
Mean	80.90	Adjusted R^2	0.9776
C.V. %	1.26	Predicted R^2	0.9330
		Adeq Precision	32.5927

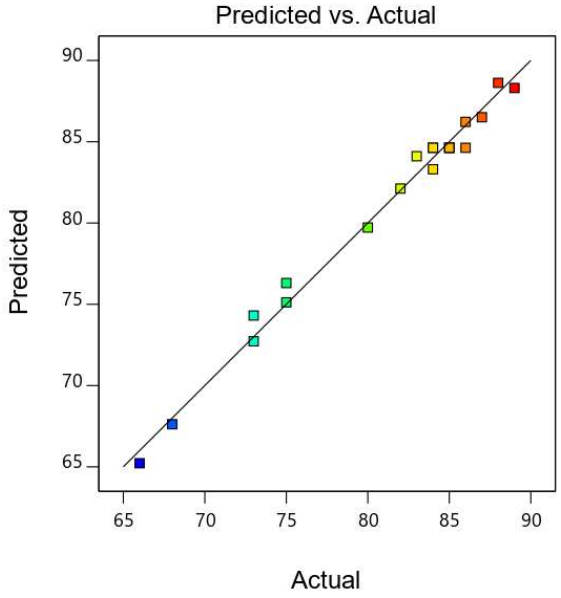

Figure 3.50- Predicted vs actual plots for gold leaching

Finally, in order to gain better understanding of the interaction effects of variables on the leaching of gold, 3-dimensional response surface plots and 2-dimensional contour plots were drawn as shown in **Figure 3.51.** These show that the leaching efficiency of gold increases with increasing the residence time and stirring speed. However, as the temperature increases, gold leaching efficiency increases until 60 °C and then decreases. Therefore numerical optimization of parameters of RSM was chosen for the maximum leaching efficiency. The blue colour indicates the lowest leaching and the red colour indicates the highest leaching in **Figure 3.51.**

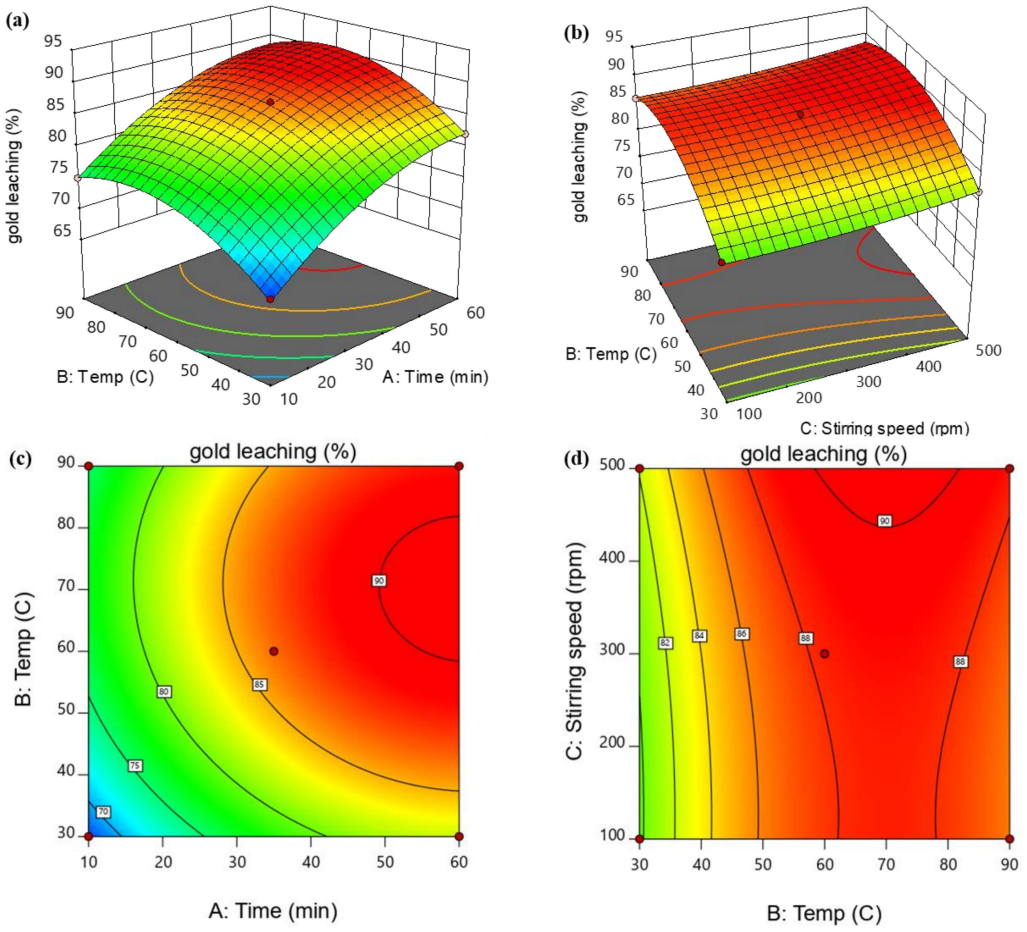

Figure 3.51- Three-dimensional response surface plots and two- dimensional contour plots for the leaching of gold [(a) and (c) represents at a constant stirring speed of 500 rpm, (b) and (d) represents at constant time of 1 h]

RSM optimization of parameters showed that the quantitative leaching of gold (90.7%) was seen at 60 min, at 70 °C temperature and at 499 rpm stirring speed as depicted in **Figure 3.52**.

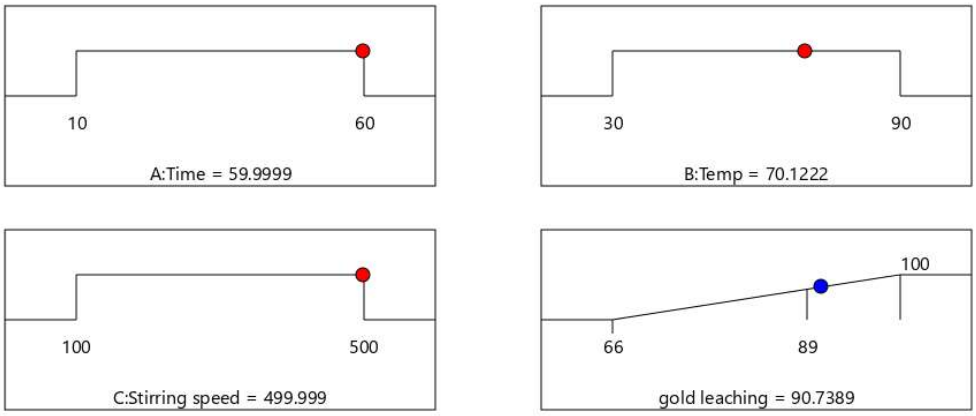

Figure 3.52- Optimization of parameters for the leaching of gold

By comparing these data with the experimental optimizations, a similar effect was again seen on gold leaching in the mentioned range of parameters. Thus, the DOE approach has validated the experimental data as elucidated in **section 3.1**, and clearly established optimal conditions without additional classical experimental optimization.

Conclusions

- Leaching of copper, nickel and gold was obtained in two stages were validated with response surface methodology.
- RSM optimization of parameters showed that the quantitative leaching of copper and nickel was seen at 120 min, using 2.9 M nitric acid, and at 490 rpm stirring speed at 30 °C temperature and 50 g/L pulp density in stage-1 leaching.
- Maximum leaching of gold (90.7%) was observed at 60 min, at 70 °C, and at 499 rpm stirring speed in stage-2 leaching with 3 M sulfuric acid combined with 3 M sodium bromide.

- By comparing these data with the experimental optimization mentioned in section 3.1, an almost similar effect was seen on copper, nickel and gold leaching in the mentioned range of parameters.
- DOE approach clearly established that optimal conditions were met without further classical experimental optimization.
- The new optimization method (RSM) not only saved experimental time but also minimized the use and loss of chemicals inherent to conventional experimental processes.